A spectroscopic study of the 14NH radical in vibrationally excited levels of the X 3Σ- state by far-infrared laser magnetic resonance

Andrew Robinson, John M. Brown, Jesus Flores-Mijangos, Lyndon Zink, Michael Jackson

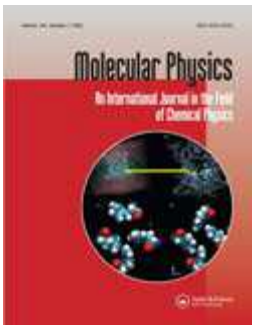

A spectroscopic study of the ^{14}NH radical in vibrationally excited levels of the $X\,^3\Sigma^-$ state by far-infrared laser magnetic resonance

Journal:	*Molecular Physics*
Manuscript ID:	TMPH-2006-0082.R1
Manuscript Type:	Full Paper
Date Submitted by the Author:	03-Dec-2006
Complete List of Authors:	Robinson, Andrew; University of Oxford, Physical and Theoretical Chemistry Laboratory Brown, John; University of Oxford, Physical and Theoretical Chemistry Laboratory Flores-Mijangos, Jesus; Universidad Nacional Autónoma de México, Instituto de Ciencias Nucleares Zink, Lyndon; University of Wisconsin-La Crosse, Department of Physics Jackson, Michael; University of Wisconsin-La Crosse, Department of Physics
Keywords:	|*bsup*|14|*esup*|NH radical, far-infrared laser magnetic resonance (LMR), magnetic hyperfine parameters, optically pumped molecular laser, Zeeman effect

MOLECULAR PHYSICS, Vol. X, No. X, Month 2006, xxx-xxx

Keywords: ^{14}NH radical, far-infrared laser magnetic resonance (LMR); Zeeman effect; magnetic hyperfine parameters; optically pumped molecular laser.
AMS Subject classification: 92E99

1 Introduction

The imidogen (NH) radical is of fundamental importance and thus has been subject to a significant number of experimental and theoretical spectroscopic investigations. For example, the band structure of the $A\ ^3\Pi$–$X\ ^3\Sigma^-$ system, which falls in the ultraviolet near 336 nm, was first studied by Eder in 1893 [1]. The accuracy of subsequent measurements with the addition of new bands was greatly improved in 1986 by Brazier *et al*. [2] using a Fourier transform spectrometer (FTS). Likewise, beginning with the initial investigations of the $c\ ^1\Pi$–$a\ ^1\Delta$ system at 324 nm in the 1930s [for example, refs. 3 and 4], recent high-resolution measurements performed by laser-induced fluorescence molecular beam experiments [5] and FTS experiments [6] have allowed the Λ-doubling interaction to be determined for the excited $a\ ^1\Delta$ state.

Along with playing a significant role in many chemical processes, including combustion [7], NH has been investigated in a variety of stellar environments such as stars, comets and diffuse clouds by monitoring the $A\ ^3\Pi$–$X\ ^3\Sigma^-$ transition [8 – 11]. With the advent of infrared astronomy, vibration-rotation lines of NH have also been detected [12 – 17] as well as pure rotation lines at far-infrared wavelengths [18]. The first laboratory based vibration-rotation spectra of NH were recorded in 1982 by Bernath and Amano [19]. This study recorded the vibrational fundamental of the $X\ ^3\Sigma^-$ ground state. Recently this work has been extended by the investigation of the first five vibration-rotation bands in the $\Delta v = 1$ sequence [20]. In 1985 Hall *et al*. [21] observed the vibrational fundamental of the excited $a\ ^1\Delta$ state by colour centre laser kinetic spectroscopy.

The intrinsic frequency tuning of laser magnetic resonance (LMR), complemented by a large database of fixed frequency far-infrared laser lines, provided a powerful technique for studying pure rotation transitions. Radford and Litvak [22] in 1975 observed the $N = 1 \leftarrow 0$ rotational transition of ^{14}NH ($X\ ^3\Sigma^-$, $v = 0$). Wayne and Radford [23] then investigated ^{14}NH ($X\ ^3\Sigma^-$, $v = 0$ and 1) with the observation of the isotopic forms ^{15}NH ($X\ ^3\Sigma^-$, $v = 0$) and ^{14}ND ($X\ ^3\Sigma^-$, $v = 0$ and 1). In 1986, Leopold *et al*. [24] observed the rotational spectra of the excited $a\ ^1\Delta$ state of ^{14}NH and ^{14}ND with LMR. Tunable far-infrared radiation has also been used to study the zero-field pure rotation spectra of ^{14}NH in $X\ ^3\Sigma^-$, $v = 0$ from $N = 1 \leftarrow 0$ to $5 \leftarrow 4$ [25 – 28].

In this paper, the prior LMR studies of ^{14}NH have been extended to include higher rotational intervals in the $v = 1$ and 2 levels in the $X\ ^3\Sigma^-$ electronic state. This work provides an improved set of molecular parameters, particularly for the $v = 2$ hyperfine coupling constants which have been experimentally determined for the first time. Only absorption lines with fully resolved hydrogen and nitrogen hyperfine structure have been included in the fit. The refined parameters will further aid astrophysical work in which the NH radical is employed as an interstellar probe.

2 Experimental Apparatus

The far-infrared laser magnetic resonance spectrometer, shown in figure 1, was designed and developed in the Boulder laboratories of the National Institute of Standards and Technology by Evenson and co-workers [29, 30]. Briefly, the NH radical is simultaneously subjected to a time-varying magnetic field and a beam of fixed-frequency laser radiation generated by an optically pumped molecular laser [31]. The far-infrared laser operates between 30 and 1000 μm; the laser lines used in this work are listed in Table 1. The far-infrared laser cavity consists of two parts, the gain region and the sample region. In the gain region, a suitable gas (e.g. CH_3OH) is pumped nearly transversely (13^o to 17^o off of transverse) by a continuous wave CO_2 laser with a power output near 30 W. The resultant far-infrared radiation oscillates in the laser cavity, defined by a fixed mirror at one end and a movable mirror attached to a micrometer drive at the other. Using a nearly confocal mirror geometry, the far-infrared laser operates on a single frequency that is known to a few parts in 10^7. An iris near the movable mirror is used to eliminate off-axis modes.

Figure 1. The far-infrared laser cavity within the magnetic resonance spectrometer system.

Table 1. Summary of the far-infrared LMR spectra of the ^{14}NH radical in the v = 1 and 2 levels of the $X\,^3\Sigma^-$ state.

The gain cell of the far-infrared laser is separated from the sample region of the cavity by a 13 μm thick polypropylene window, set at the Brewster angle. This window serves two purposes: (i) it provides the vacuum seal between the gain cell and the sample region of the cavity, and (ii) it restricts the polarisation of the laser to a single linear configuration, which can be oriented either parallel (π; $\Delta M_J = 0$, $E \parallel B_Z$) or perpendicular (σ; $\Delta M_J = \pm 1$, $E \perp B_Z$) to the magnetic field. The sample region of the laser cavity is positioned between the pole faces of an electromagnet operating with an 8 cm air gap, capable of generating magnetic fields up to 2.0 T. A set of Helmholtz coils mounted on the laser cavity provides the modulation field; in this experiment it was operated at 5.901 kHz. A fraction of the laser radiation is coupled out of the cavity using a movable 45^o copper mirror. The far-infrared radiation passes through a teflon window and is focused on a detector using an off-axis parabolic mirror. Resonance signals, detected with a gallium-doped germanium bolometer cooled to 2 K, were processed by a lock-in amplifier at the modulation frequency and recorded with a computer as a function of flux density. The magnetic field measurements were calibrated with a NMR gaussmeter and are reported with experimental uncertainties varying from 0.13 to 0.3 mT, depending on the signal-to-noise ratio of the absorption lines.

The NH radicals were produced in the sample region by the reaction of fluorine atoms with NH_3 in a flow system. The fluorine atoms were generated by passing a mixture of He (at 119 Pa) with 5% F_2 in helium (at 14 Pa) through a 12 W microwave discharge, produced using an Evenson cavity [34]. The total pressure in the sample volume was about 133 Pa with trace amounts of NH_3 added downstream. This resulted in pushing the reaction zone down into the laser beam, generating larger signals. Higher amounts of NH_3 (pressures above 0.5 Pa) would result in the generation of both NH and NH_2.

3 Theory

The far-infrared LMR spectra of the NH radical can be conveniently described by an effective Hamiltonian that operates only within the spin-rotational manifold of a vibrational level for a given electronic state [35]. The operator for a molecule in a $^3\Sigma^-$ state is well-established [23] and can be written as

$$H_{\text{eff}} = H_{\text{rot}} + H_{\text{fs}} + H_{\text{hfs}} + H_{\text{zee}}. \tag{1}$$

Here H_{rot} is the standard rotational Hamiltonian

$$H_{\text{rot}} = B_v \boldsymbol{N}^2 - D_v \boldsymbol{N}^4 + H_v \boldsymbol{N}^6 + \ldots \tag{2}$$

and H_{fs} is the fine-structure operator

$$H_{\text{fs}} = \tfrac{2}{3}\lambda_v (3S_z^2 - \boldsymbol{S}^2) + \gamma_v \boldsymbol{N}\cdot\boldsymbol{S} + \tfrac{1}{2}\gamma_{Dv}[(\boldsymbol{N}\cdot\boldsymbol{S}), \boldsymbol{N}^2]_+ + \ldots ; \tag{3}$$

here z is the internuclear axis, defining the orientation of the molecule-fixed axis system in laboratory space.

Both ^{1}H (I_{H} = ½) and ^{14}N (I_{N} = 1) nuclei show hyperfine interactions that are resolved in high resolution spectra. The larger contribution arises from magnetic hyperfine interactions. For a molecule in a $^3\Sigma^-$ state

$$H_{\text{hfs}} = \sum_k b_{Fk} \boldsymbol{I}_k \cdot \boldsymbol{S} + \sum_k \frac{c_k}{3}\left(3I_{zk}S_z - \boldsymbol{I}_k \cdot \boldsymbol{S}\right) \tag{4}$$

where k labels the nucleus in question. The parameter b_{Fk} describes the Fermi contact interaction and c_k describes the axial dipolar interaction; c is related to the hyperfine t parameter by $t = c/3$ [35]. The ^{14}N nucleus also shows an electric quadrupole interaction (that produces a slight asymmetry in the hyperfine splitting in the LMR spectra). This is represented for the ^{14}N nucleus by

$$H_{\text{Q}} = \frac{eq_0 Q}{4I(2I-1)}\left(3I_Z^2 - \boldsymbol{I}^2\right) \tag{5}$$

The effects of the external magnetic field in the LMR experiment are described by the Zeeman Hamiltonian. For a molecule in a $^3\Sigma^-$ state exposed to a flux density B_Z

$$H_{\text{zee}} = g_S \mu_B \boldsymbol{B}\cdot\boldsymbol{S} + g_\ell^e \mu_B (B_x S_x + B_y S_y) - g_r \mu_B \boldsymbol{B}\cdot\boldsymbol{N} + \sum_k g_k \mu_N \left(\boldsymbol{B}\cdot\boldsymbol{I}_k\right) \qquad (6)$$

Here g_S is the electron spin g-factor and g_l^e is its anisotropic correction, arising from the axial symmetry of the diatomic molecule; g_r is the rotational g-factor and g_N the nuclear spin g-factor. The Zeeman effect is dominated by the g_S term.

The zero-field Hamiltonian can be used to construct an energy level diagram for the first few rotational levels of the NH radical, using the parameters given in Table 2. The diagram for the v = 1 level of NH is shown in figure 2. Some typical LMR transitions are indicated, showing some of the laser lines used in the present work.

The matrix representation of the effective Hamiltonian H_{eff} in Eqn. (1) is constructed in a Hund's case (b), nuclear spin-decoupled basis set $|\, \eta\, \Lambda;\, N\, S\, J\, M_J;\, I_H\, M_H;\, I_N\, M_N\rangle$. This is appropriate since the nuclear hyperfine interactions are much smaller than the Zeeman interaction in our experiments. The Zeeman Hamiltonian, Eqn. (6), has matrix elements in this basis set ΔN = 0, ±2 and ΔJ = 0, ±1 and so the matrix representation is strictly of infinite dimension. In practice, it is truncated at a certain level of ΔN so that it reproduces the eigenvalues to better than experimental accuracy. The calculation of the eigenvalues and eigenvectors was performed using a computer program. The program exploits the fact that the rotational levels of a molecule in a Σ^- state have parity $-(-1)^N$ and treats the matrix representations of the even (E) and odd (O) parity states separately. The ΔN = 0, and ΔJ = ±1 matrix elements of the Zeeman Hamiltonian cause J to cease being a good quantum number in the magnetic field. The eigenstates are therefore labelled by parity, M_J and an energy-ordering index, counting from the highest state downwards; this index is obviously basis-set dependent.

Table 2. Molecular parameters for ^{14}NH in the v = 0, 1 and 2 levels of the $X\,^3\Sigma^-$ state.[a]

Figure 2. Diagram showing the lower energy levels of the ^{14}NH radical in the v = 1 level of the $X\,^3\Sigma^-$ state. ΔN = +1 and ΔJ = +1 transitions are shown with several corresponding FIR laser lines that could be used to study each rotational interval. The energy separation of the fine structure components is exaggerated for clarity.

4 Spectra and Analysis

4.1 Observations and Assignments

Resonance signals associated with the first four rotational intervals have been observed for the $v = 1$ level while resonance signals in the first three rotational intervals have been observed for the $v = 2$ level. Figure 3 shows part of the 160.448 μm spectrum for the $v = 1$ level while Figure 4 shows part of the 166.631 μm spectrum for the $v = 2$ level. Here the Zeeman components of the $N = 2 \leftarrow 1$ transition are shown. The magnetic hyperfine structure associated with the ^{1}H ($I = 1/2$) and ^{14}N ($I = 1$) nuclei is clearly visible. The NH_2 radical could also be formed in the chemical reaction used to produce NH. The signals from these two species can be distinguished by their characteristic hyperfine patterns and by simple chemical tests. Although a few of the NH signals showed overlap of the hyperfine structure, the majority of the signals showed fully resolved hyperfine structure.

Figure 3. Part of the far-infrared LMR spectrum of the ^{14}NH radical in the $v = 1$ level of the $X\ ^{3}\Sigma^{-}$ state. The spectrum is recorded with the 160.448 μm laser line in the parallel polarisation ($\Delta M_J = 0$). The rotational transitions involved are $N = 2 \leftarrow 1$, $M_J = 2 \leftarrow 2$ and $M_J = 0 \leftarrow 0$. The ^{1}H and ^{14}N hyperfine structures are both fully resolved; the nuclear spin selection rule is $\Delta M_I = 0$.

Figure 4. Part of the far-infrared LMR spectrum of the ^{14}NH radical in the $v = 2$ level of the $X\ ^{3}\Sigma^{-}$ state. The spectrum is recorded with the 166.631 μm laser line in the perpendicular polarisation ($\Delta M_J = \pm 1$). The rotational transition involved is $N = 2 \leftarrow 1$, $M_J = 0 \leftarrow 1$. The ^{1}H and ^{14}N hyperfine structures are both fully resolved; the nuclear spin selection rule is $\Delta M_I = 0$.

Within the field range covered in the LMR experiments, the electron spin becomes decoupled from the molecular framework and the Zeeman effect becomes quite complex. Assignments were made by comparison with predictions of the computer program, which has the capability of calculating the relative intensities and tuning rates of each transition. A typical Zeeman tuning pattern is shown in figure 5. The tuning rate is particularly useful information and can assist in making specific assignments by de-tuning the wavelength of the far-infrared laser slightly. For example, the transition labelled e in figure 5 tunes positively whereas f tunes negatively. A subset of the measured individual resonance

signals observed in the LMR spectra of vibrationally excited ^{14}NH are given in Table 3 together with their assignments.

Table 3. Several observed LMR absorption lines for ^{14}NH assigned to transitions in the v = 1 and 2 levels of the $X\,^3\Sigma^-$ state.

Figure 5. This diagram illustrates the tuning of the $\Delta M_J = 0, \pm 1$ transitions between the Zeeman manifolds for $N = 2 \leftarrow 1$ and $\Delta J = +1$ (pseudo selection rule) in the $v = 1$ level of ^{14}NH. Coincidences can be seen with both the 158.513 μm and 160.448 μm laser lines. The labelled transitions ($M_J' \leftarrow M_J''$) for the 158.513 μm line are a: $-1 \leftarrow -2$, b: $0 \leftarrow -1$, c: $-1 \leftarrow -1$, d: $-1 \leftarrow -1$, e: $0 \leftarrow -1$, f: $1 \leftarrow 0$, and for the 160.448 μm line A: $1 \leftarrow 2$, B: $2 \leftarrow 2$, C: $0 \leftarrow 1$.

4.2 Determination of Molecular Parameters

The data for ^{14}NH in each vibrational level were fit by a least-squares procedure to determine the appropriate parameters of the effective Hamiltonian given in Eqn. (1). Each data point was weighted as the inverse square of its experimental uncertainty, that is based on the uncertainty in the magnetic field, the tuning rate and the uncertainty in the far-infrared laser frequency. Because our measurements are confined to low N-values, we have constrained the centrifugal distortion parameters H_v and γ_{Dv} to the values determined in a recent infrared study [20]. In addition, the ^{14}N electric quadrupole interaction had a marginal effect on the spectra; this parameter was therefore constrained to the value determined recently for the $v = 0$ level [27].

A total of 357 data points were included in the fit for the $v = 1$ level resulting in a standard deviation relative to the estimated experimental uncertainty of 0.29. For the $v = 2$ level, 360 data points were fit with a standard deviation of 0.30. The parameters determined in the process are given in Table 4. A value of 1.0 is expected if the model Hamiltonian is adequate and the weight factors of the individual transitions have been chosen correctly. This result indicates the reported experimental uncertainties might be slightly overestimated, probably arising from the errors reported for the magnetic field measurements.

Table 4. Comparison of molecular parameters for ^{14}NH in the $X\,^3\Sigma^-$ state.[a]

5 Discussion

The rotational spectrum of the ^{14}NH radical has been studied in the v = 1 and 2 levels of its $X\,^3\Sigma^-$ state by far-infrared laser magnetic resonance. Extensive observations have been made, much of it showing full hyperfine structure. This has allowed the determination of an accurate set of parameters in the effective Hamiltonian. These vibration-rotation levels have been studied previously through electronic spectroscopy [2] and most recently (and accurately) through its infrared spectrum [20]. The rotational and fine-structure parameters determined in the latter study are compared with those of the present work in Table 4. It can be seen that we have achieved an improvement in accuracy by an order of magnitude for the fine-structure parameters. The reason for this is that the far-infrared LMR experiment provides accurate measurements of the lowest N-transitions in the spectrum. The spin-spin parameter λ shows only a weak dependence on v; this is expected because the open-shell pair of electrons are located on the N atom and their interaction is insensitive to the N–H bond length. By contrast, the spin-rotation parameter γ depends quite strongly on v; the moment of inertia of ^{14}NH depends directly on the bond length.

Part of the motivation for this study was to provide the spectroscopic information for radio astronomers to detect vibrationally excited ^{14}NH in the interstellar medium. To this end, we provide the transition frequencies for the first five rotational transitions of ^{14}NH in the v = 1 and 2 levels, together with their relative intensities in Table 5. For the sake of simplicity, we have not included the nuclear hyperfine structure; such effects produce a structure on each rotational transition with a spread of a few MHz [27].

Table 5. Computed zero-field frequencies for the first five rotational intervals in the v = 1 and 2 levels of the $X\,^3\Sigma^-$ state in ^{14}NH.

The high resolution of the far-infrared LMR experiment has permitted the full determination of the magnetic hyperfine parameters for ^{14}NH in the v = 1 and 2 levels for the first time. The values are collected in Table 6, together with the earlier result for the v = 0 level obtained by sub-millimeter wave and tunable far-infrared spectroscopy [27, 28]. The two parameters concerned, b_F (Fermi contact) and c (the axial dipolar interaction) represent the expectation values of well-established operators [23, 35] and provide direct information on the electronic wavefunction in the immediate neighbourhood of the nucleus concerned. There have been several *ab initio* calculations of these hyperfine parameters for ^{14}NH; these are also listed in Table 6. One of the earliest, by Kristiansen and Veseth [38], used many-body perturbation theory. This gave excellent agreement with the experimental results and in some respects rendered subsequent calculations superfluous. Other calculations have in fact used the ^{14}NH results as a benchmark against which to test their wavefunctions. That by Engels and Peyerimhoff [39] investigated the effect of polarisation on configuration interaction while Fernández *et al*. [40] used a modern, complete active space valence (CASV) multiconfiguration SCF approach. For all these calculations, the agreement with

experiment is good, in part reflecting the comparative simplicity of the wavefunction for ^{14}NH in its $X\,^3\Sigma^-$ state.

Table 6. Comparison of magnetic nuclear hyperfine parameters for ^{14}NH in the $X\,^3\Sigma^-$ state.[a]

Turning to the experimental results in Table 6, it can be seen that some of the hyperfine parameters show a stronger vibrational dependence than others. Both the ^{1}H and ^{14}N Fermi contact parameters show a distinct trend with v. This behaviour occurs because both these interactions depend on spin-polarisation, particularly for the proton (hence its sign). Such effects are very sensitive to the nature of the electronic wavefunction, which is changed subtly by extension of the N–H bond length. For the dipolar parameters on the other hand, c barely changes at all with v for ^{14}N while it shows a distinct trend for ^{1}H. This reflects the nature of the open-shell π orbital that is located on the ^{14}N atom and contains both electrons. The separation of the unpaired electrons from the ^{14}N nucleus does not change during the vibration. On the other hand, the proton is separated from the electrons by the bond length and so is directly affected by vibrational averaging.

One of the major achievements of the present work is that we have been able to determine a full set of Zeeman parameters for ^{14}NH in its v = 1 and 2 levels. This has been rarely achieved for other free radicals (not even, for example, for O_2 [41]). It results from multiple observations of a given rotational transition with different laser lines, so providing a direct measurement of magnetic tuning rates. None of the three g-factors, given in Table 2, show a significant vibrational dependence. The average value for g_S is accurately determined to be 2.002 131(61), different from the free-spin value of 2.002 319 by a small but significant amount. The difference is –0.188 × 10^{-3} or 94 ppm and is largely attributable to the relativistic mass correction [35]. This correction is almost in exact agreement with the value calculated by Wayne and Radford using a good SCF wavefunction [23]. The average value determined for g_l^e, the anisotropic correction to g_S, is 0.1600(81) × 10^{-2}. This agrees well with the expectations of Curl's formula [37]

$$g_l^e = -\gamma_v / 2B_v \qquad (7)$$

which predicts an average value of 0.1643 × 10^{-2} from the parameters given in Table 2. Finally, we come to the rotational g-factor, g_r. This parameter has two contributions, nuclear and electronic

$$g_r = g_r^N - g_r^e \qquad (8)$$

The nuclear part depends only on the charges and masses of the nuclei [35] and is readily calculated to be 0.5262 × 10^{-3} for ^{14}NH. Hence the average electronic contribution, g_r^e, is determined to be 0.2027(18) × 10^{-2} for ^{14}NH in its $X\,^3\Sigma^-$ state. In the effective Hamiltonian, g_r^e arises from the admixture of excited electronic states into the ground state through

rotational motion [35]. The contribution from the $A\ ^3\Pi$ state at 29761 cm^{-1} is approximately $4B/(E_\Pi - E_\Sigma)$ or 0.220×10^{-2} for ^{14}NH. This effectively explains the experimental value and supports the suggestion that the A and X states are in "pure precession".

This paper presents a detailed study of the molecular and magnetic properties of the ^{14}NH radical in vibrationally excited levels and is the first experimental investigation of the magnetic hyperfine structure in the $v = 2$ level for ^{14}NH in the $X\ ^3\Sigma^-$ state. We are in the process of studying ^{14}ND, ^{15}NH and ^{15}ND by far-infrared LMR, extending this investigation to its isotopic forms. These isotopic forms of NH may be used as molecular probes in the interstellar medium. For example, an accurate set of experimentally determined molecular parameters for ^{15}NH would permit the relative abundances of ^{14}N and ^{15}N to be determined in regions of star formation, providing information on this process.

Acknowledgments

We wish to dedicate this paper to our former friend and colleague, Ken Evenson, who passed away in 2002. He was the inventor of the Laser Magnetic Resonance method and developed the technique to a high level of sophistication. Following his death, his apparatus was moved to its present location at the University of Wisconsin – La Crosse and re-commissioned. The work reported in this paper is the first piece of research carried out with the apparatus. We remain indebted to Ken and inspired to carry on the work he initiated.

The authors are pleased to acknowledge the following programs for their financial support: the National Science Foundation (Grant Nos. RUI-0604715 and OISE-0200746), the Wisconsin Space Grant Consortium (Research Infrastructure Program), the CSAH Faculty Sabbatical Program and the Dirección General de Asuntos del Personal Académico (DGAPA-UNAM for project IN 120906-3). The authors would also like to thank A. Cooksy for his assistance with the DIAT computer program.

References

For Placement on the Web

Supplemental Table A. Details of the observed resonance signals and the least-squares fit for the $v = 1$ level of the $X\,^3\Sigma^-$ state in ^{14}NH.

Supplemental Table B. Details of the observed resonance signals and the least-squares fit for the $v = 2$ level of the $X\,^3\Sigma^-$ state in ^{14}NH.

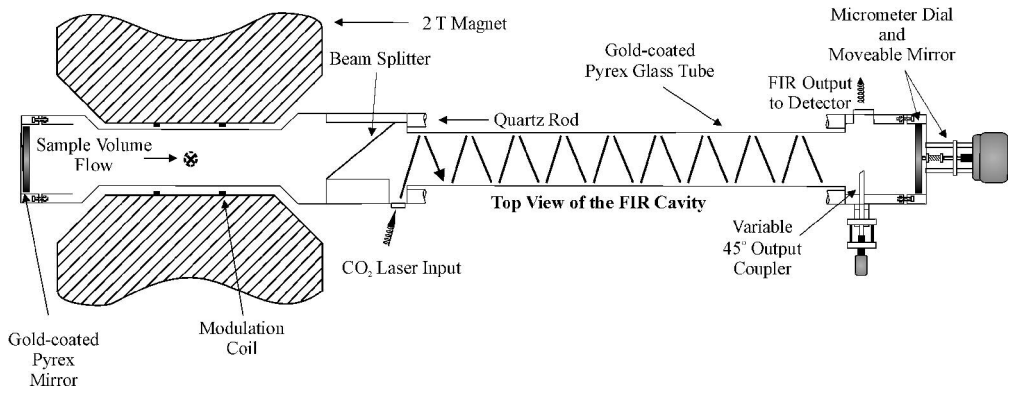

The far-infrared laser cavity within the magnetic resonance spectrometer system.

$N' \leftarrow N''$	FIR Laser Medium	CO_2 Pump	λ (μm)	Wavenumber (cm^{-1})	Frequency (MHz)	Ref.
1 ← 0	N_2H_4	10*R*12	373.577	26.7683	802 492.8 ± 0.2[a]	32
	N_2H_4	10*P*56	338.516	29.5407	885 606.8 ± 0.2[a,b]	32
	CH_2DOH	9*P*12	322.452	31.0123	929 726.8 ± 0.5[a,b]	33
	N_2H_4	9*P*46	312.027	32.0485	960 791.1 ± 0.2[a,b]	32
	CH_2DOH	9*P*14	308.040	32.4633	973 224.3 ± 0.5[a,b]	33
	N_2H_4	10*R*12	301.275	33.1922	995 077.8 ± 0.5[a]	33
2 ← 1	$^{13}CH_3OH$	10*R*18	171.758	58.2216	1 745 439.5 ± 0.9[a]	33
	CH_2F_2	9*R*22	166.677	59.9964	1 798 647.0 ± 0.9[a]	33
	CH_2F_2	9*R*20	166.631	60.0128	1 799 139.3 ± 0.9[a,b]	33
	CH_3OH	10*R*38	163.034	61.3371	1 838 839.3 ± 1.0[a,b]	33
	N_2H_4	9*P*46	160.448	62.3256	1 868 475.5 ± 0.4[a,b]	32
	CH_2F_2	9*P*10	158.513	63.0861	1 891 274.3 ± 1.0[b]	33
3 ← 2	$^{13}CH_3OH$	10*R*18	110.432	90.5531	2 714 714.7 ± 1.4[a]	33
	CH_2F_2	9*P*24	109.296	91.4948	2 742 946.0 ± 1.4[a,b]	33
	CH_2DOH	9*P*12	108.818	91.8968	2 754 995.7 ± 1.4[a,b]	33
	$^{13}CH_3OH$	10*R*18	105.147	95.1048	2 851 169.2 ± 1.5[b]	33
4 ← 3	N_2H_4	9*R*8	81.099	123.3066	3 696 638.2 ± 0.8[b]	32

[a] Used to observe absorption lines in the $v = 2$ level.
[b] Used to observe absorption lines in the $v = 1$ level.

Parameters	$v = 0$ Ref. [27]	$v = 1$ [Present work]	$v = 2$ [Present work]
B_v	489 959.076 8(40)[b]	470 566.753(35)	451 201.878 (51)
D_v	51.051 11(33)	50.344 6(21)	49.809 1(38)
$H_v \times 10^3$	3.737 6(72)	3.520 9[c]	3.330[c]
λ_v	27 577.848(11)	27 564.77(18)	27 517.95(21)
λ_{Dv}	0.010 3(24)		
γ_v	–1 644.486 0(72)	–1 557.823(51)	– 1 471.387(50)
γ_{Dv}	0.451 81(30)	0.420 5[c]	0.399 0[c]
b_F (^{1}H)	– 66.131(15)	– 68.92(18)	– 74.18(21)
c (^{1}H)[d]	90.291(84)	88.77(99)	85.5(10)
C_I (^{1}H)	– 0.061(23)		
b_F (^{14}N)	18.830(10)	17.71(11)	17.17(12)
c (^{14}N)[d]	– 67.922(29)	– 67.56(64)	– 67.26(63)
eq_0Q (^{14}N)	– 2.883(62)	– 2.883[e]	– 2.883[e]
C_I (^{14}N)	0.145 5(89)		
g_S		2.002 166(44)	2.002 095(42)
$g_l^e \times 10^2$		0.154 3(58)	0.165 6(57)
$g_r \times 10^2$		– 0.150 84(98)	– 0.149 3(15)
g_n (^{1}H)[f]		5.585 690	5.585 690
g_n (^{14}N)[f]		0.403 761	0.403 761

[a] The values of the parameters are given in MHz, apart from the g-factors.
[b] The figures in parenthesis represent one standard deviation of the least-squares fit of the experimental data, in units of the last quoted decimal place.
[c] Parameter constrained to this value from Ref. [20] in the least-squares fit.
[d] The axial dipolar interaction c is related to the hyperfine t parameter by $t = c/3$ [35].
[e] Parameter constrained to the $v = 0$ value [27] in the least-squares fit.
[f] Value quoted in nuclear magnetons [36].

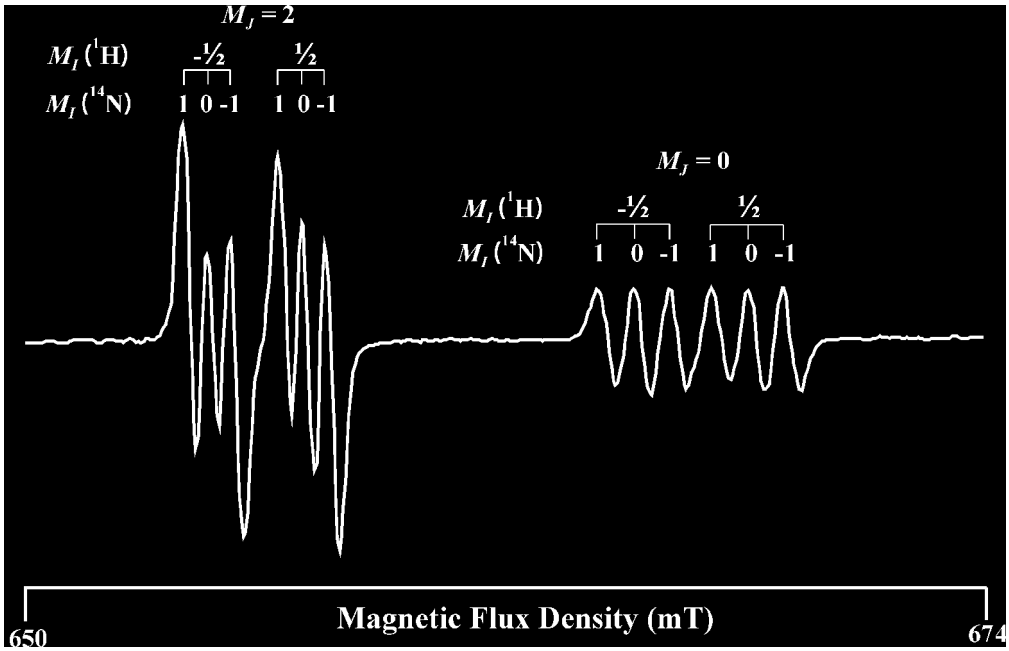

Part of the far-infrared LMR spectrum of the ^{14}NH radical in the υ = 1 level of the $X\,^3\Sigma^-$ state. The spectrum is recorded with the 160.448 μm laser line in the parallel polarisation ($\Delta M_J = 0$). The rotational transitions involved are $N = 2 \leftarrow 1$, $M_J = 2 \leftarrow 2$ and $M_J = 0 \leftarrow 0$. The ^{1}H and ^{14}N hyperfine structures are both fully resolved; the nuclear spin selection rule is $\Delta M_I = 0$.

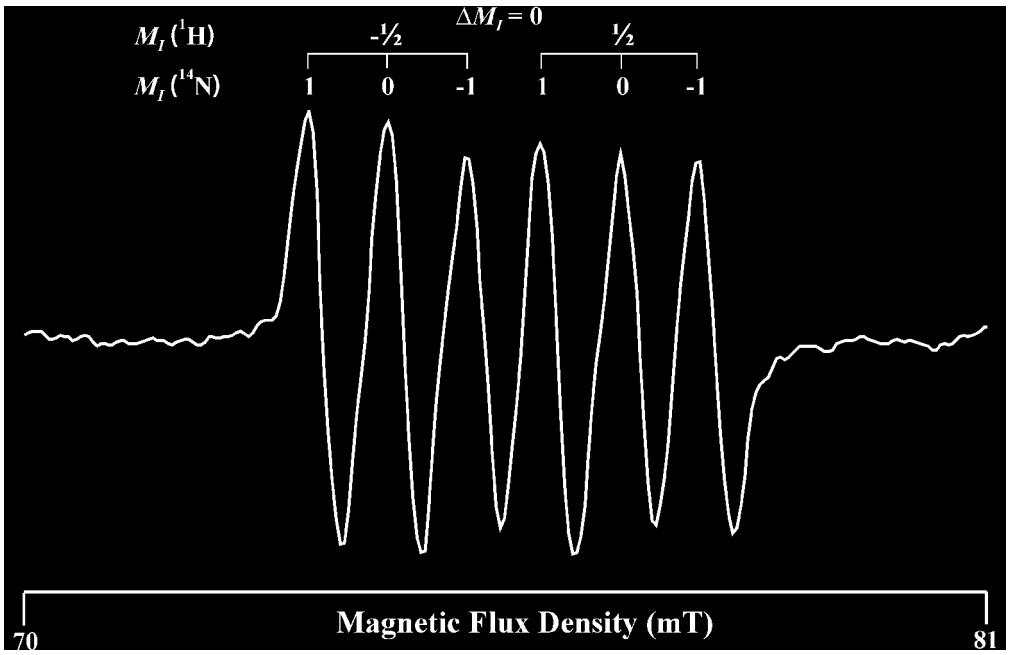

Part of the far-infrared LMR spectrum of the ^{14}NH radical in the $v = 2$ level of the $X\,^3\Sigma^-$ state. The spectrum is recorded with the 166.631 μm laser line in the perpendicular polarisation ($\Delta M_J = \pm 1$). The rotational transition involved is $N = 2 \leftarrow 1$, $M_J = 0 \leftarrow 1$. The ^{1}H and ^{14}N hyperfine structures are both fully resolved; the nuclear spin selection rule is $\Delta M_I = 0$.

M_I (^{1}H)[a]	M_I (^{14}N)[a]	M_J'	M_J''	Flux Density (mT)	Tuning Rate (MHz/mT)	Obs. – Calc. (MHz)
N: 2 ← 1; v = 1; π polarisation				ν_{laser} = 1 868 475.5 ± 0.4 MHz		
–0.5	1	2	2	654.11	–18.47	–0.22
–0.5	0	2	2	654.68	–18.46	0.08
–0.5	–1	2	2	655.18	–18.45	–0.69
0.5	1	2	2	656.49	–18.46	0.68
0.5	0	2	2	656.99	–18.45	–0.36
0.5	–1	2	2	657.56	–18.44	0.21
–0.5	1	0	0	664.46	–14.05	0.30
–0.5	0	0	0	665.34	–14.04	0.60
–0.5	–1	0	0	666.27	–14.07	0.27
0.5	1	0	0	667.37	–14.05	0.44
0.5	0	0	0	668.22	–14.09	–0.57
0.5	–1	0	0	669.08	–14.07	–1.01
N: 2 ← 1; v = 2; σ polarisation				ν_{laser} = 1 799 139.3 ± 0.9 MHz		
–0.5	1	1	2	53.84	–19.80	0.14
–0.5	0	1	2	54.71	–19.85	–0.50
–0.5	–1	1	2	55.61	–19.86	0.82
0.5	1	1	2	56.40	–19.71	–0.07
0.5	0	1	2	57.32	–19.76	0.30
0.5	–1	1	2	58.19	–19.78	1.07
–0.5	1	0	1	73.27	–14.47	0.29
–0.5	0	0	1	74.21	–14.47	0.04
–0.5	–1	0	1	75.19	–14.49	0.82
0.5	1	0	1	76.05	–14.43	0.24
0.5	0	0	1	77.04	–14.44	0.72
0.5	–1	0	1	77.97	–14.45	0.80
–0.5	1	–1	–2	102.34	39.45	–0.37
–0.5	0	–1	–2	103.74	39.41	0.07
–0.5	–1	–1	–2	105.24	39.37	–1.96
0.5	1	–1	–2	105.98	39.38	–2.02
0.5	0	–1	–2	107.36	39.40	–0.77
0.5	–1	–1	–2	108.84	39.36	–1.99

[a] Note that ΔM_I (^{1}H) = 0 and ΔM_I (^{14}N) = 0.

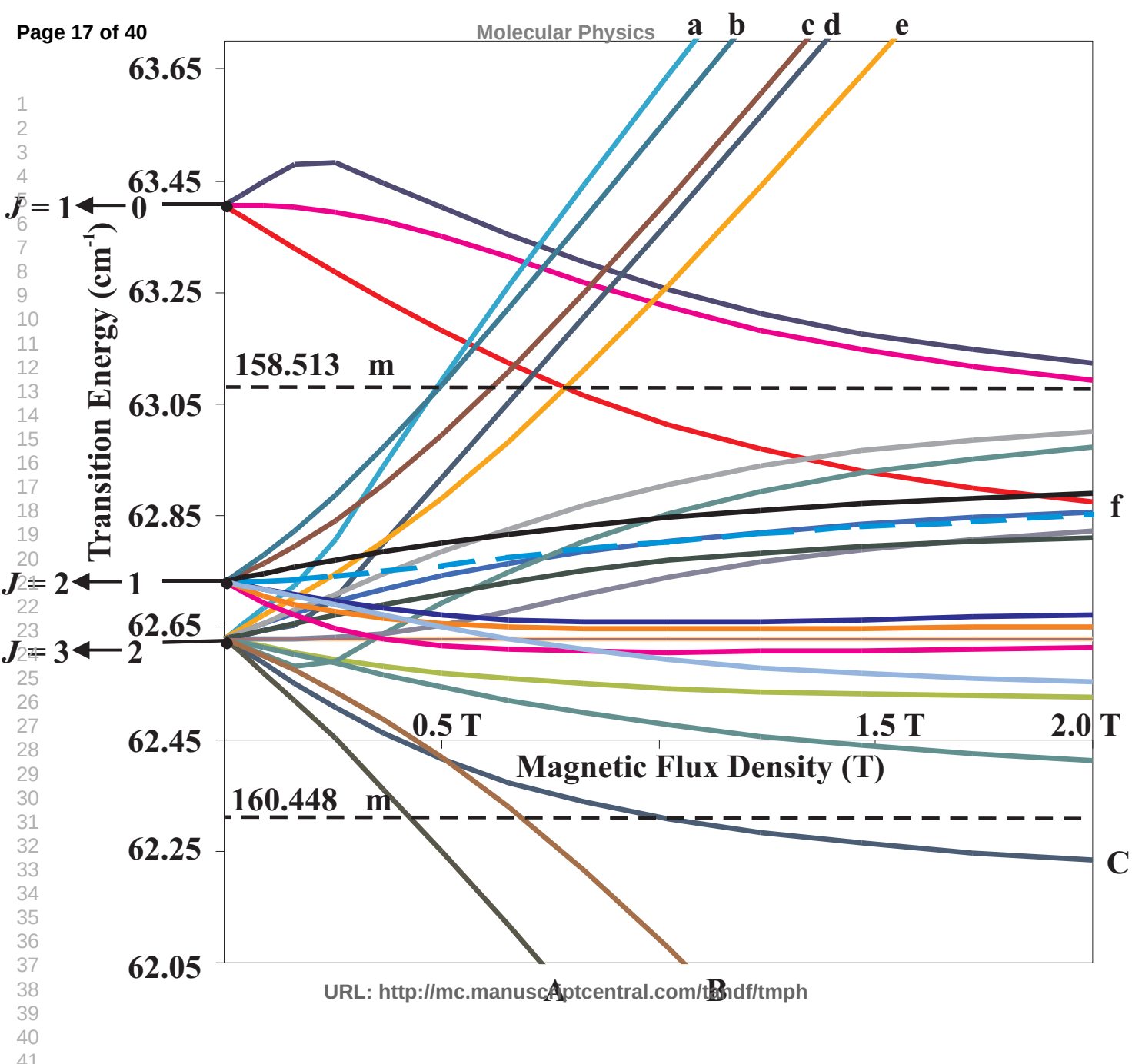
a
b
c
d
e
63.65
63.45
63.25
63.05
62.85
62.65
62.45
62.25
62.05
J = 1
J = 2
J = 3
0
1
2
Transition Energy (cm-1)
158.513 m
160.448 m
f
C
0.5 T
1.5 T
2.0 T
Magnetic Flux Density (T)
A
B

Parameter	Present work		Ram *et al*. [20]	
	$v = 1$	$v = 2$	$v = 1$	$v = 2$
B_v	15.696 417 3(12) [b]	15.050 474 6(17)	15.696 430 2(40)	15.050 538 1(84)
$D_v \times 10^3$	1.679 315(70)	1.661 45(13)	1.679 475(28)	1.661 615(65)
$H_v \times 10^7$	1.174 46[c]	1.110 8[c]	1.174 46[c]	1.110 8[c]
λ_v	0.919 461 8(60)	0.917 900 0(70)	0.919 96(13)	0.918 45(24)
$\gamma_v \times 10^2$	– 5.196 34(17)	– 4.908 02(17)	– 5.178 4(14)	– 4.882 1(25)
$\gamma_{Dv} \times 10^5$	1.402 5[c]	1.330 8[c]	1.402 5[c]	1.330 8[c]

[a] The values of the parameters are given in cm^{-1}.

[b] The figures in parenthesis represent one standard deviation of the least-squares fit of the experimental data, in units of the last quoted decimal place.

[c] Parameter constrained to this value from Ref. [20] in the least-squares fit.

$N' \leftarrow N''$	$J' \leftarrow J''$	$v = 1$ $\nu_{transition}$ (MHz)	$v = 2$ $\nu_{transition}$ (MHz)	Line Strengths
$1 \leftarrow 0$	$0 \leftarrow 1$	907 534	868 705	0.34
	$2 \leftarrow 1$	935 785	897 153	1.67
	$1 \leftarrow 1$	961 106	922 270	0.99
$2 \leftarrow 1$	$1 \leftarrow 1$	1 847 253	1 769 710	0.51
	$3 \leftarrow 2$	1 877 570	1 800 218	2.80
	$2 \leftarrow 1$	1 880 655	1 803 213	1.50
	$1 \leftarrow 0$	1 900 826	1 823 275	0.66
	$2 \leftarrow 2$	1 905 976	1 828 330	0.50
$3 \leftarrow 2$	$4 \leftarrow 3$	2 815 570	2 699 527	3.86
	$3 \leftarrow 2$	2 817 966	2 701 835	2.67
	$2 \leftarrow 1$	2 823 104	2 706 877	1.80
$4 \leftarrow 3$	$5 \leftarrow 4$	3 749 587	3 594 891	4.89
	$4 \leftarrow 3$	3 751 665	3 596 882	3.75
	$3 \leftarrow 2$	3 754 737	3 599 864	2.86
$5 \leftarrow 4$	$6 \leftarrow 5$	4 678 659	4 485 361	5.91
	$5 \leftarrow 4$	4 680 558	4 487 174	4.80
	$4 \leftarrow 3$	4 682 937	4 489 465	3.89

	$b_F(^1H)$	$c(^1H)$	$b_F(^{14}N)$	$c(^{14}N)$	Ref.
			Experimental values		
$v = 0$	– 66.131(15)[b]	90.291(84)	18.830(10)	– 67.922(29)	[27]
$v = 1$	– 68.92(18)	88.77(99)	17.71(11)	– 67.56(64)	this work
$v = 2$	– 74.18(21)	85.5(10)	17.17(12)	– 67.26(63)	this work
			Theoretical values (*at* R_e)		
MBPT	– 66.35	91.95	18.94	– 66.99	[38]
MRD-CI	– 64.5	93.6	19	– 68.1	[39]
CASV	– 66.23	91.71	19.22	– 67.92	[40]

[a] The values of the parameters are given in MHz.

[b] The figures in parenthesis represent one standard deviation of the least-squares fit of the experimental data, in units of the last quoted decimal place.

References

[1] J. M. Eder. *Denksch. Wien. Akad.*, **60**, 1 (1893)
[2] C. R. Brazier, R. S. Ram, and P. F. Bernath. *J. molec. Spectrosc.*, **120**, 381 (1986)
[3] R. W. B. Pearse. *Proc. R. Soc. London, Ser. A*, **143**, 112 (1933)
[4] G. H. Dieke and R. W. Blue. *Phys. Rev.*, **45**, 395 (1934)
[5] W. Ubachs, G. Meyer, J. J. Ter Meulen, and A. Dymanus. *J. molec. Spectrosc.*, **115**, 88 (1986)
[6] R. S. Ram and P. F. Bernath. *J. opt. Soc. Am. B*, **3**, 1170 (1986)
[7] W. Hack. NH radical reactions, review article in: Z. B. Zlfassi (Ed.), N-Centered Radicals, Wiley, Chicester, 413 (1998).
[8] J. L. Schmitt. *Publ. Astron. Soc. Pacific*, **81**, 657 (1969)
[9] R. W. Shaw. *Astrophys. J.*, **83**, 225 (1936)
[10] P. Swings, C. T. Elvey, and H. W. Babcock. *Astrophys. J.*, **94**, 320 (1941)
[11] M. M. Litvak and E. N. R. Kuiper. *Astrophys. J.*, **253**, 622 (1982)
[12] D. M. Meyer and K. C. Roth. *Astrophys. J.*, **376**, L49 (1991)
[13] D. L. Lambert and R. Beer. *Astrophys. J.*, **177**, 541 (1972)
[14] D. L. Lambert, J. A. Brown, K. H. Hinkle, and H. R. Johnson. *Astrophys. J.*, **284**, 223 (1984)
[15] S. T. Ridgway, D. F. Carbon, D. N. B. Hall, and J. Jewell. *Astrophys. J. Suppl. Ser.*, **54**, 177 (1984)
[16] N. Grevesse, D. L. Lambert, and A. J. Sauval. *Astron. Astrophys.*, **232**, 225 (1990)
[17] D. L. Lambert, B. Gustafsson, K. Erikson, and K. H. Hinkle. *Astrophys. J. Suppl. Ser.*, **62**, 373 (1986)
[18] M. Geller, A. J. Sauval, N. Grevesse, C. B. Farmer, and R. H. Norton. *Astron. Astrophys.*, **249**, 550 (1991)
[19] P. F. Bernath and T. Amano. *J. molec. Spectrosc.*, **95**, 359 (1982)
[20] R. S. Ram, P. F. Bernath, and K. H. Hinkle. *J. chem. Phys.*, **110**, 5557 (1999)
[21] J. L. Hall, H. Adams, J. V. V. Kasper, R. F. Curl, and F. K. Tittel. *J. opt. Soc. Am. B*, **2**, 781 (1985)
[22] H. E. Radford and M. M. Litvak. *Chem. Phys. Lett.*, **34**, 561 (1975)
[23] F. D. Wayne and H. E. Radford. *Mol. Phys.*, **32**, 1407 (1976)
[24] K. R. Leopold, K. M. Evenson, and J. M. Brown. *J. chem. Phys.*, **85**, 324 (1986)
[25] F. C. Van der Heuvel, W. L. Meerts, and A. Dymanus. *Chem. Phys. Lett.*, **92**, 215 (1982)
[26] T. Klaus, S. Takano, and G. Winnewisser. *Astron. Astrophys.*, **322**, L1 (1997)
[27] J. Flores-Mijangos, J. M. Brown, F. Matsushima, H. Odashima, K. Takagi, L. R. Zink, and K. M. Evenson. *J. molec. Spectrosc.*, **225**, 189 (2004)
[28] F. Lewen, S. Brunken, G. Winnewisser, M. Simeckova, and S. Urban. *J. molec. Spectrosc.*, **226**, 113 (2004)
[29] K. M. Evenson, R. J. Saykally, D. A. Jennings, R. F. Curl Jr., and J. M. Brown. "Far Infrared Laser Magnetic Resonance," in Chemical and Biochemical Applications of Lasers, Volume V, C. Bradley Moore, Ed., 95 (1980)

[30] T. J. Sears, P. R. Bunker, A. R. W. McKellar, K. M. Evenson, D. A. Jennings, and J. M. Brown. *J. chem. Phys.*, **77**, 5348 (1982)
[31] N. G. Douglas. Millimetre and Submillimetre Wavelength Lasers: A Handbook of CW Measurements, Springer, New York (1989)
[32] A. De Michele, G. Carelli, G. Moruzzi, and A. Moretti. *J. opt. Soc. Am. B*, **22**, 1461 (2005)
[33] M. Inguscio, G. Moruzzi, K. M. Evenson, and D.A. Jennings. *J. appl. Phys.*, **60**, 161 (1986)
[34] F. C. Fehsenfeld, K. M. Evenson, and H. P. Broida. *Rev. Sci. Instrum.*, **36**, 294 (1965)
[35] J. M. Brown and A. Carrington. *Rotational Spectroscopy of Diatomic Molecules*, Cambridge University Press, Cambridge (2003)
[36] I. M. Mills, T. Cvitas, K. Homann, N. Kallay, and K. Kuchitsu. *Quantities, Units and Symbols in Physical Chemistry*, 2nd Ed. (International Union of Pure and Applied Chemistry), Blackwell Scientific Publishing, Oxford (1993)
[37] R. F. Curl. *Mol. Phys.*, **9**, 585 (1965)
[38] P. Kristiansen and L. Veseth. *J. chem. Phys.*, **84**, 6336 (1986)
[39] B. Engels and S. D. Peyerimhoff. *Mol. Phys.*, **67**, 583 (1989)
[40] B. Fernández, P. Jørgensen, E. A. McCullough, and J. Simons. *J. chem. Phys.*, **99**, 5995 (1993)
[41] M. Tinkham and M. W. P. Strandberg. *Phys. Rev.*, **97**, 951 (1955)

Line	ODD		EVEN		B (mT)	ν_{Laser} (MHz)	Weight	O – C (MHz)
	M_F[a]	Eigenstate[b]	M_F[a]	Eigenstate[c]				
1	-0.5	40	-0.5	58	650.51	973224.3	0.0880	-0.46
2	-1.5	37	-1.5	53	651.81	973224.3	0.0879	-0.09
3	-2.5	33	-2.5	45	653.16	973224.3	0.0878	-0.38
4	0.5	41	0.5	58	653.91	973224.3	0.0879	-0.95
5	-0.5	41	-0.5	57	655.21	973224.3	0.0878	0.12
6	-1.5	38	-1.5	52	656.51	973224.3	0.0877	0.16
7	0.5	39	0.5	56	898.10	973224.3	0.0923	-0.37
8	-0.5	38	-0.5	55	898.90	973224.3	0.0923	-0.71
9	-1.5	36	-1.5	51	899.65	973224.3	0.0923	-0.71
10	1.5	38	1.5	53	900.73	973224.3	0.0924	-0.28
11	0.5	40	0.5	57	901.56	973224.3	0.0923	-1.13
12	-0.5	39	-0.5	56	902.29	973224.3	0.0924	-0.87
13	-0.5	37	-1.5	51	652.19	973224.3	0.0878	0.04
14	0.5	37	-0.5	55	652.63	973224.3	0.0878	-1.31
15	1.5	37	0.5	57	653.66	973224.3	0.0878	1.42
16	2.5	33	1.5	53	654.21	973224.3	0.0878	-1.19
17	0.5	45	-0.5	58	1581.99	973224.3	0.0245	-3.37
18	-0.5	43	-1.5	53	1582.92	973224.3	0.0245	-3.57
19	-1.5	39	-2.5	45	1583.92	973224.3	0.0245	0.65
20	1.5	43	0.5	58	1584.87	973224.3	0.0245	1.42
21	0.5	46	-0.5	57	1585.82	973224.3	0.0245	5.43
22	-0.5	44	-1.5	52	1586.82	973224.3	0.0245	4.97
23	0.5	39	-0.5	58	348.08	973224.3	0.0303	-0.94
24	-0.5	38	-1.5	53	348.72	973224.3	0.0303	0.45
25	-1.5	36	-2.5	45	349.39	973224.3	0.0303	-0.16
26	1.5	38	0.5	58	350.59	973224.3	0.0303	-1.38
27	0.5	40	-0.5	57	351.30	973224.3	0.0303	-2.75
28	-0.5	39	-1.5	52	351.95	973224.3	0.0303	-2.67
29	2.5	34	2.5	41	654.11	1868475.5	0.1299	-0.22
30	1.5	39	1.5	43	654.68	1868475.5	0.1300	0.08
31	0.5	42	0.5	43	655.18	1868475.5	0.1301	-0.69
32	3.5	27	3.5	36	656.49	1868475.5	0.1300	0.68
33	2.5	35	2.5	42	656.99	1868475.5	0.1301	-0.36
34	1.5	40	1.5	44	657.56	1868475.5	0.1302	0.21
35	0.5	45	0.5	51	664.46	1868475.5	0.2066	0.30
36	-0.5	43	-0.5	51	665.34	1868475.5	0.2068	0.60
37	-1.5	39	-1.5	47	666.27	1868475.5	0.2061	0.27
38	1.5	43	1.5	48	667.37	1868475.5	0.2066	0.44
39	0.5	46	0.5	50	668.22	1868475.5	0.2056	-0.57
40	-0.5	44	-0.5	50	669.08	1868475.5	0.2061	-1.01
41	0.5	45	1.5	50	288.42	1868475.5	0.1607	-0.26
42	-0.5	43	0.5	53	290.78	1868475.5	0.1607	-0.55
43	0.5	46	1.5	49	295.75	1868475.5	0.1607	-0.93

44	-0.5	44	0.5	52	298.28	1868475.5	0.1607	-0.74
45	2.5	34	1.5	45	407.24	1868475.5	0.0764	-2.47
46	1.5	39	0.5	44	408.05	1868475.5	0.0764	-0.78
47	0.5	42	-0.5	43	408.73	1868475.5	0.0764	-0.91
48	3.5	27	2.5	43	409.83	1868475.5	0.0764	-0.92
49	2.5	35	1.5	46	410.59	1868475.5	0.0764	-0.51
50	1.5	40	0.5	45	411.30	1868475.5	0.0764	0.13
51	0.5	45	-0.5	49	738.45	1868475.5	0.1581	-0.64
52	-0.5	43	-1.5	46	739.15	1868475.5	0.1578	-0.06
53	-1.5	39	-2.5	40	739.87	1868475.5	0.1578	-0.93
54	1.5	43	0.5	49	741.00	1868475.5	0.1576	-1.49
55	0.5	46	-0.5	48	741.72	1868475.5	0.1575	-2.25
56	-0.5	44	-1.5	45	742.44	1868475.5	0.1576	-1.51
57	1.5	41	0.5	47	884.13	1868475.5	0.0980	-0.49
58	0.5	43	-0.5	46	886.37	1868475.5	0.0980	0.97
59	1.5	42	0.5	48	890.17	1868475.5	0.0980	0.36
60	0.5	44	-0.5	47	891.66	1868475.5	0.0980	-0.11
61	1.5	36	1.5	50	257.52	1838839.3	0.0312	-1.59
62	0.5	37	0.5	53	258.07	1838839.3	0.0312	-1.43
63	-0.5	37	-0.5	53	258.69	1838839.3	0.0311	-1.51
64	2.5	33	2.5	44	259.96	1838839.3	0.0312	-1.21
65	1.5	37	1.5	49	260.53	1838839.3	0.0311	-1.34
66	0.5	38	0.5	52	261.11	1838839.3	0.0311	-1.77
67	0.5	39	0.5	47	878.33	1838839.3	0.0703	1.01
68	-0.5	38	-0.5	46	879.05	1838839.3	0.0703	0.66
69	-1.5	36	-1.5	44	879.68	1838839.3	0.0703	0.27
70	1.5	38	1.5	47	880.84	1838839.3	0.0703	0.60
71	0.5	40	0.5	48	881.61	1838839.3	0.0703	1.22
72	-0.5	39	-0.5	47	882.26	1838839.3	0.0704	1.42
73	1.5	41	1.5	50	1172.90	1838839.3	0.0180	0.31
74	0.5	43	0.5	53	1174.36	1838839.3	0.0179	-0.74
75	-0.5	42	-0.5	53	1175.88	1838839.3	0.0179	-0.68
76	2.5	36	2.5	44	1176.47	1838839.3	0.0179	-1.17
77	1.5	42	1.5	49	1178.13	1838839.3	0.0179	3.45
78	0.5	44	0.5	52	1179.67	1838839.3	0.0179	4.14
79	2.5	34	2.5	41	1923.49	1838839.3	0.0210	-3.05
80	1.5	39	1.5	43	1924.23	1838839.3	0.0210	-2.74
81	0.5	41	0.5	43	1924.98	1838839.3	0.0210	-2.67
82	3.5	27	3.5	36	1926.15	1838839.3	0.0210	-1.48
83	2.5	35	2.5	42	1926.89	1838839.3	0.0210	-1.44
84	1.5	40	1.5	44	1927.66	1838839.3	0.0210	-0.57
85	0.5	39	1.5	50	349.78	1838839.3	0.0236	0.71
86	-0.5	38	0.5	53	351.10	1838839.3	0.0235	0.19
87	-1.5	36	-0.5	53	352.42	1838839.3	0.0234	-0.38
88	1.5	38	2.5	44	353.18	1838839.3	0.0234	0.51

89	0.5	40	1.5	49	354.50	1838839.3	0.0233	0.03
90	-0.5	39	0.5	52	355.87	1838839.3	0.0234	1.16
91	0.5	39	-0.5	49	537.27	1838839.3	0.0306	0.66
92	-0.5	38	-1.5	46	537.82	1838839.3	0.0306	0.01
93	-1.5	36	-2.5	40	538.36	1838839.3	0.0306	0.37
94	1.5	38	0.5	49	539.65	1838839.3	0.0306	2.27
95	0.5	40	-0.5	48	540.19	1838839.3	0.0306	0.78
96	-0.5	39	-1.5	45	540.76	1838839.3	0.0307	2.79
97	-0.5	37	-1.5	44	642.19	1838839.3	0.0637	-0.70
98	0.5	37	-0.5	46	642.67	1838839.3	0.0636	0.21
99	1.5	37	0.5	48	643.68	1838839.3	0.0638	-1.64
100	2.5	33	1.5	47	644.14	1838839.3	0.0637	-1.20
101	2.5	34	1.5	50	705.86	1838839.3	0.0173	0.22
102	1.5	39	0.5	53	707.08	1838839.3	0.0173	1.16
103	0.5	41	-0.5	53	708.23	1838839.3	0.0173	-1.78
104	3.5	27	2.5	44	709.07	1838839.3	0.0173	-0.26
105	2.5	35	1.5	49	710.31	1838839.3	0.0173	1.66
106	1.5	40	0.5	52	711.49	1838839.3	0.0173	0.35
107	-0.5	40	0.5	51	1072.27	1838839.3	0.0299	3.70
108	-1.5	37	-0.5	51	1073.19	1838839.3	0.0299	3.30
109	-2.5	33	-1.5	47	1074.14	1838839.3	0.0298	1.40
110	0.5	42	1.5	48	1075.13	1838839.3	0.0298	0.94
111	-0.5	41	0.5	50	1076.07	1838839.3	0.0298	-2.29
112	-1.5	38	-0.5	50	1076.97	1838839.3	0.0298	-2.04
113	0.5	39	1.5	45	1104.34	1838839.3	0.0266	0.61
114	-0.5	38	0.5	44	1104.90	1838839.3	0.0266	1.08
115	-1.5	36	-0.5	43	1105.36	1838839.3	0.0266	0.57
116	1.5	38	2.5	43	1106.62	1838839.3	0.0266	0.33
117	0.5	40	1.5	46	1107.17	1838839.3	0.0266	0.42
118	-0.5	39	0.5	45	1107.66	1838839.3	0.0266	0.76
119	2.5	34	1.5	45	1499.85	1838839.3	0.0186	-0.03
120	1.5	39	0.5	44	1500.60	1838839.3	0.0186	-1.27
121	0.5	41	-0.5	43	1501.36	1838839.3	0.0186	-0.94
122	3.5	27	2.5	43	1502.45	1838839.3	0.0186	-1.07
123	2.5	35	1.5	46	1503.26	1838839.3	0.0186	-0.81
124	1.5	40	0.5	45	1504.05	1838839.3	0.0186	0.51
125	0.5	45	1.5	50	1774.92	1838839.3	0.0227	0.51
126	-0.5	43	0.5	53	1776.50	1838839.3	0.0227	0.75
127	-1.5	39	-0.5	53	1778.18	1838839.3	0.0227	0.27
128	1.5	43	2.5	44	1778.67	1838839.3	0.0227	-0.61
129	0.5	46	1.5	49	1780.28	1838839.3	0.0227	-0.06
130	-0.5	44	0.5	52	1781.96	1838839.3	0.0227	-0.08
131	-0.5	46	-0.5	44	688.15	1891274.3	0.0517	0.33
132	-1.5	41	-1.5	42	689.23	1891274.3	0.0517	0.42
133	-2.5	34	-2.5	39	690.29	1891274.3	0.0516	0.97

134	0.5	47	0.5	46	691.17	1891274.3	0.0516	0.86
135	-0.5	45	-0.5	45	692.25	1891274.3	0.0516	1.68
136	-1.5	40	-1.5	43	693.29	1891274.3	0.0515	1.95
137	0.5	49	1.5	50	759.28	1891274.3	0.0671	0.51
138	-0.5	49	0.5	53	760.98	1891274.3	0.0669	0.83
139	0.5	48	1.5	49	764.86	1891274.3	0.0669	0.74
140	-0.5	48	0.5	52	766.58	1891274.3	0.0670	0.56
141	-0.5	46	0.5	47	793.93	1891274.3	0.0651	-0.01
142	-1.5	41	-0.5	46	794.45	1891274.3	0.0651	-0.48
143	-2.5	34	-1.5	44	794.91	1891274.3	0.0651	1.54
144	0.5	47	1.5	47	796.23	1891274.3	0.0651	0.82
145	-0.5	45	0.5	48	796.73	1891274.3	0.0651	1.98
146	-1.5	40	-0.5	47	797.28	1891274.3	0.0651	0.81
147	-2.5	22	-2.5	44	214.87	2851169.2	0.0519	0.05
148	-3.5	19	-3.5	36	216.53	2851169.2	0.0519	-0.36
149	-4.5	15	-4.5	27	218.31	2851169.2	0.0044	-3.20
150	-1.5	24	-1.5	50	218.57	2851169.2	0.0044	1.53
151	-2.5	23	-2.5	43	220.28	2851169.2	0.0518	0.02
152	-3.5	20	-3.5	35	221.94	2851169.2	0.0517	-0.16
153	-1.5	22	-1.5	48	240.38	2851169.2	0.0446	1.15
154	-2.5	20	-2.5	42	241.51	2851169.2	0.0446	0.82
155	-3.5	18	-3.5	34	242.63	2851169.2	0.0445	0.30
156	-0.5	24	-0.5	50	243.45	2851169.2	0.0446	-0.05
157	-1.5	23	-1.5	47	244.52	2851169.2	0.0444	1.12
158	-2.5	21	-2.5	41	245.66	2851169.2	0.0445	0.04
159	-1.5	22	-2.5	44	177.56	2851169.2	0.0355	1.42
160	-2.5	20	-3.5	36	178.77	2851169.2	0.0355	2.18
161	-3.5	18	-4.5	27	180.09	2851169.2	0.0354	0.82
162	-0.5	24	-1.5	49	180.82	2851169.2	0.0355	1.16
163	-1.5	23	-2.5	43	182.03	2851169.2	0.0354	1.89
164	-2.5	21	-3.5	35	183.35	2851169.2	0.0354	0.48
165	-0.5	22	-1.5	48	208.68	2851169.2	0.0375	3.69
166	-1.5	20	-2.5	42	209.64	2851169.2	0.0373	2.09
167	-2.5	19	-3.5	34	210.52	2851169.2	0.0373	3.20
168	0.5	24	-0.5	50	211.50	2851169.2	0.0373	2.00
169	-0.5	23	-1.5	47	212.40	2851169.2	0.0373	2.10
170	-1.5	21	-2.5	41	213.35	2851169.2	0.0373	1.15
171	0.5	29	1.5	50	1333.74	2851169.2	0.0183	0.59
172	-0.5	29	0.5	53	1335.00	2851169.2	0.0183	0.94
173	-1.5	29	-0.5	53	1336.37	2851169.2	0.0183	0.78
174	1.5	30	2.5	44	1337.13	2851169.2	0.0183	0.14
175	0.5	30	1.5	49	1338.41	2851169.2	0.0183	-0.02
176	-0.5	30	0.5	52	1339.76	2851169.2	0.0183	0.30
177	0.5	45	-0.5	58	1079.89	960791.1	0.0937	-2.38
178	-0.5	43	-1.5	53	1080.88	960791.1	0.0936	-2.97

179	-1.5	39	-2.5	45	1081.92	960791.1	0.0937	-1.76
180	1.5	43	0.5	58	1082.84	960791.1	0.0936	-0.94
181	0.5	46	-0.5	57	1083.81	960791.1	0.0937	0.60
182	-0.5	44	-1.5	52	1084.89	960791.1	0.0936	-0.76
183	2.5	32	2.5	37	890.84	2754995.7	0.0178	-2.26
184	1.5	35	1.5	39	891.56	2754995.7	0.0178	-0.91
185	0.5	36	0.5	40	892.27	2754995.7	0.0178	-3.04
186	3.5	26	3.5	33	893.43	2754995.7	0.0178	-2.45
187	2.5	31	2.5	38	894.17	2754995.7	0.0178	-1.59
188	1.5	34	1.5	41	894.91	2754995.7	0.0178	-0.87
189	-0.5	34	-0.5	40	1063.70	2754995.7	0.0067	1.91
190	-1.5	32	-1.5	38	1064.34	2754995.7	0.0067	3.40
191	-2.5	27	-2.5	36	1064.90	2754995.7	0.0067	-1.95
192	0.5	33	0.5	42	1066.14	2754995.7	0.0067	-0.86
193	-0.5	33	-0.5	41	1066.78	2754995.7	0.0067	-4.33
194	-1.5	31	-1.5	39	1067.41	2754995.7	0.0067	-1.66
195	-0.5	26	-0.5	40	1959.76	2754995.7	0.0054	2.72
196	-1.5	27	-1.5	38	1960.65	2754995.7	0.0054	3.16
197	-2.5	26	-2.5	36	1961.46	2754995.7	0.0054	3.20
198	0.5	26	0.5	42	1962.55	2754995.7	0.0054	4.05
199	-0.5	27	-0.5	41	1963.43	2754995.7	0.0054	3.92
200	-1.5	28	-1.5	39	1964.22	2754995.7	0.0054	3.74
201	2.5	32	1.5	37	864.55	2754995.7	0.0164	3.31
202	1.5	35	0.5	37	865.30	2754995.7	0.0164	3.41
203	0.5	36	-0.5	37	866.11	2754995.7	0.0164	2.84
204	3.5	26	2.5	36	867.22	2754995.7	0.0164	3.14
205	2.5	31	1.5	38	868.00	2754995.7	0.0164	3.69
206	1.5	34	0.5	38	868.76	2754995.7	0.0164	1.72
207	1.5	33	0.5	39	964.69	2754995.7	0.0165	-2.58
208	0.5	35	-0.5	38	965.30	2754995.7	0.0165	-0.99
209	-0.5	35	-1.5	37	965.93	2754995.7	0.0165	-0.10
210	2.5	30	1.5	39	967.17	2754995.7	0.0165	-0.11
211	1.5	32	0.5	40	967.75	2754995.7	0.0165	-1.16
212	0.5	34	-0.5	39	968.36	2754995.7	0.0165	-0.08
213	1.5	33	2.5	37	970.04	2754995.7	0.0179	0.09
214	0.5	35	1.5	40	970.41	2754995.7	0.0179	0.56
215	-0.5	35	0.5	41	970.81	2754995.7	0.0179	0.19
216	2.5	30	3.5	33	972.19	2754995.7	0.0179	-0.24
217	1.5	32	2.5	38	972.56	2754995.7	0.0179	-1.88
218	0.5	34	1.5	41	972.93	2754995.7	0.0179	-1.51
219	0.5	33	1.5	39	974.31	2754995.7	0.0065	0.18
220	-0.5	33	0.5	40	974.71	2754995.7	0.0065	-1.56
221	-1.5	31	-0.5	39	975.06	2754995.7	0.0065	-1.43
222	0.5	32	-0.5	40	1092.36	2754995.7	0.0064	6.70
223	-0.5	32	-1.5	38	1092.99	2754995.7	0.0064	8.12

224	-1.5	30	-2.5	36	1093.53	2754995.7	0.0064	1.71
225	1.5	31	0.5	42	1094.80	2754995.7	0.0064	3.59
226	0.5	31	-0.5	41	1095.41	2754995.7	0.0064	-1.20
227	-0.5	31	-1.5	39	1095.97	2754995.7	0.0064	-1.61
228	0.5	29	-0.5	40	1852.14	2754995.7	0.0055	-1.73
229	-0.5	29	-1.5	38	1853.15	2754995.7	0.0055	-1.59
230	-1.5	29	-2.5	36	1854.08	2754995.7	0.0055	-1.57
231	1.5	30	0.5	42	1855.07	2754995.7	0.0055	-1.04
232	0.5	30	-0.5	41	1856.09	2754995.7	0.0055	-0.96
233	-0.5	30	-1.5	39	1856.98	2754995.7	0.0055	-1.66
234	2.5	32	2.5	37	1140.09	2742946.0	0.0061	0.09
235	1.5	35	1.5	40	1140.79	2742946.0	0.0061	0.52
236	0.5	36	0.5	41	1141.54	2742946.0	0.0061	-0.19
237	3.5	26	3.5	33	1142.67	2742946.0	0.0061	-1.02
238	2.5	31	2.5	38	1143.42	2742946.0	0.0061	-0.01
239	1.5	34	1.5	41	1144.15	2742946.0	0.0061	0.20
240	2.5	32	1.5	37	1103.33	2742946.0	0.0057	-0.58
241	1.5	35	0.5	37	1104.07	2742946.0	0.0057	0.23
242	0.5	36	-0.5	37	1104.86	2742946.0	0.0057	-0.58
243	3.5	26	2.5	36	1105.97	2742946.0	0.0057	-1.11
244	2.5	31	1.5	38	1106.73	2742946.0	0.0057	-0.83
245	1.5	34	0.5	38	1107.47	2742946.0	0.0057	-2.63
246	1.5	33	0.5	39	1203.79	2742946.0	0.0057	-1.08
247	0.5	35	-0.5	38	1204.38	2742946.0	0.0057	0.38
248	-0.5	35	-1.5	37	1204.95	2742946.0	0.0057	-1.83
249	2.5	30	1.5	39	1206.20	2742946.0	0.0057	-1.82
250	1.5	32	0.5	40	1206.75	2742946.0	0.0057	-4.51
251	0.5	34	-0.5	39	1207.35	2742946.0	0.0057	-3.07
252	0.5	32	-0.5	40	1335.30	2742946.0	0.0000	7.85
253	-0.5	32	-1.5	38	1335.94	2742946.0	0.0000	9.26
254	-1.5	30	-2.5	36	1336.53	2742946.0	0.0059	0.09
255	1.5	31	0.5	42	1337.74	2742946.0	0.0059	-0.49
256	0.5	31	-0.5	41	1338.40	2742946.0	0.0000	-7.82
257	-0.5	31	-1.5	39	1338.99	2742946.0	0.0000	-7.61
258	3.5	19	3.5	32	810.54	3696638.2	0.0184	-1.00
259	2.5	22	2.5	35	811.39	3696638.2	0.0184	1.11
260	1.5	24	1.5	36	812.22	3696638.2	0.0184	0.41
261	4.5	15	4.5	26	813.30	3696638.2	0.0184	0.61
262	3.5	20	3.5	31	814.13	3696638.2	0.0184	1.01
263	2.5	23	2.5	34	814.96	3696638.2	0.0184	1.14
264	2.5	20	2.5	33	815.31	3696638.2	0.0165	1.58
265	1.5	22	1.5	35	815.83	3696638.2	0.0165	1.54
266	0.5	23	0.5	35	816.35	3696638.2	0.0166	-0.50
267	3.5	18	3.5	30	817.65	3696638.2	0.0165	0.65
268	2.5	21	2.5	32	818.20	3696638.2	0.0166	0.99

269	1.5	23	1.5	34	818.74	3696638.2	0.0166	0.95
270	-1.5	22	-1.5	26	1843.85	3696638.2	0.0205	-0.93
271	-2.5	20	-2.5	27	1844.70	3696638.2	0.0205	0.11
272	-3.5	18	-3.5	26	1845.47	3696638.2	0.0205	0.80
273	-0.5	24	-0.5	25	1846.58	3696638.2	0.0205	1.06
274	-1.5	23	-1.5	27	1847.36	3696638.2	0.0205	0.17
275	-2.5	21	-2.5	28	1848.16	3696638.2	0.0205	1.70
276	2.5	20	3.5	32	764.01	3696638.2	0.0210	-5.41
277	1.5	22	2.5	35	764.81	3696638.2	0.0210	-4.29
278	0.5	23	1.5	36	765.62	3696638.2	0.0210	-5.69
279	3.5	18	4.5	26	766.73	3696638.2	0.0210	-4.48
280	2.5	21	3.5	31	767.50	3696638.2	0.0210	-5.56
281	1.5	23	2.5	34	768.32	3696638.2	0.0210	-5.69
282	1.5	19	2.5	33	799.98	3696638.2	0.0203	1.52
283	0.5	19	1.5	35	800.52	3696638.2	0.0203	0.83
284	-0.5	19	0.5	35	801.13	3696638.2	0.0203	1.05
285	2.5	19	3.5	30	802.39	3696638.2	0.0203	1.42
286	1.5	20	2.5	32	802.98	3696638.2	0.0203	2.24
287	0.5	20	1.5	34	803.59	3696638.2	0.0203	3.41
288	0.5	21	1.5	32	836.76	3696638.2	0.0072	4.59
289	-0.5	20	0.5	32	837.14	3696638.2	0.0072	4.16
290	-1.5	19	-0.5	31	837.54	3696638.2	0.0072	2.78
291	1.5	21	2.5	31	838.94	3696638.2	0.0072	4.20
292	0.5	22	1.5	31	839.34	3696638.2	0.0072	3.04
293	-0.5	21	0.5	31	839.72	3696638.2	0.0072	2.38
294	-0.5	22	0.5	34	857.94	3696638.2	0.0048	2.69
295	-1.5	20	-0.5	33	858.33	3696638.2	0.0048	2.11
296	-2.5	19	-1.5	31	858.78	3696638.2	0.0048	1.50
297	0.5	24	1.5	33	860.14	3696638.2	0.0048	1.93
298	-0.5	23	0.5	33	860.59	3696638.2	0.0048	0.60
299	-1.5	21	-0.5	32	860.96	3696638.2	0.0048	-0.33
300	3.5	19	2.5	33	866.52	3696638.2	0.0085	-2.38
301	2.5	22	1.5	35	867.08	3696638.2	0.0085	-1.27
302	1.5	24	0.5	35	867.69	3696638.2	0.0085	1.10
303	4.5	15	3.5	30	868.91	3696638.2	0.0085	-1.33
304	3.5	20	2.5	32	869.50	3696638.2	0.0085	0.03
305	2.5	23	1.5	34	870.04	3696638.2	0.0085	0.42
306	-0.5	22	0.5	29	1417.39	3696638.2	0.0133	-0.24
307	-1.5	20	-0.5	29	1418.03	3696638.2	0.0133	0.56
308	-2.5	19	-1.5	30	1418.64	3696638.2	0.0133	0.84
309	0.5	24	1.5	30	1419.87	3696638.2	0.0133	0.90
310	-0.5	23	0.5	30	1420.40	3696638.2	0.0133	-2.00
311	-1.5	21	-0.5	30	1421.10	3696638.2	0.0133	1.46
312	-1.5	22	-0.5	26	1666.72	3696638.2	0.0208	-2.44
313	-2.5	20	-1.5	28	1667.69	3696638.2	0.0208	-2.11

314	-3.5	18	-2.5	29	1668.55	3696638.2	0.0208	-2.59
315	-0.5	24	0.5	26	1669.57	3696638.2	0.0208	-2.26
316	-1.5	23	-0.5	27	1670.54	3696638.2	0.0208	-2.09
317	-2.5	21	-1.5	29	1671.45	3696638.2	0.0208	-1.05
318	1.5	36	1.5	50	1138.00	1799139.3	0.0064	4.01
319	0.5	37	0.5	53	1138.50	1799139.3	0.0064	4.35
320	-0.5	37	-0.5	53	1139.05	1799139.3	0.0064	0.87
321	2.5	33	2.5	44	1140.33	1799139.3	0.0064	0.94
322	1.5	37	1.5	49	1140.88	1799139.3	0.0064	0.05
323	0.5	38	0.5	52	1141.43	1799139.3	0.0064	0.40
324	0.5	39	0.5	51	1392.08	1799139.3	0.0064	6.10
325	-0.5	38	-0.5	51	1392.71	1799139.3	0.0064	6.75
326	-1.5	36	-1.5	47	1393.29	1799139.3	0.0064	-1.22
327	1.5	38	1.5	48	1394.54	1799139.3	0.0064	0.41
328	0.5	40	0.5	50	1395.15	1799139.3	0.0064	-7.42
329	-0.5	39	-0.5	50	1395.75	1799139.3	0.0064	-7.13
330	0.5	39	-0.5	49	1409.09	1799139.3	0.0000	13.80
331	-0.5	38	-1.5	46	1409.66	1799139.3	0.0000	15.80
332	-1.5	36	-2.5	40	1410.18	1799139.3	0.0064	3.20
333	1.5	38	0.5	49	1411.44	1799139.3	0.0064	2.76
334	0.5	40	-0.5	48	1412.00	1799139.3	0.0000	-9.37
335	-0.5	39	-1.5	45	1412.50	1799139.3	0.0000	-9.98
336	2.5	34	1.5	50	1453.01	1799139.3	0.0056	-6.37
337	1.5	39	0.5	53	1454.17	1799139.3	0.0056	-4.47
338	0.5	41	-0.5	53	1455.35	1799139.3	0.0056	-2.07
339	3.5	27	2.5	44	1456.23	1799139.3	0.0056	-0.89
340	2.5	35	1.5	49	1457.45	1799139.3	0.0056	4.01
341	1.5	40	0.5	52	1458.59	1799139.3	0.0056	4.52
342	1.5	41	1.5	51	361.33	929726.8	0.0418	0.46
343	0.5	43	0.5	54	361.59	929726.8	0.0418	-0.12
344	-0.5	42	-0.5	54	361.90	929726.8	0.0418	0.17
345	2.5	36	2.5	45	363.29	929726.8	0.0418	0.00
346	1.5	42	1.5	52	363.63	929726.8	0.0418	0.89
347	0.5	44	0.5	55	363.86	929726.8	0.0418	-0.30
348	0.5	45	1.5	51	200.01	929726.8	0.1138	-0.62
349	-0.5	43	0.5	54	200.61	929726.8	0.1138	0.07
350	-1.5	39	-0.5	54	201.15	929726.8	0.1138	-0.29
351	1.5	43	2.5	45	202.37	929726.8	0.1138	0.52
352	0.5	46	1.5	52	202.94	929726.8	0.1138	0.28
353	-0.5	44	0.5	55	203.56	929726.8	0.1138	2.47
354	-0.5	46	0.5	56	360.23	929726.8	0.1137	0.25
355	-1.5	41	-0.5	55	360.94	929726.8	0.1137	0.97
356	-2.5	34	-1.5	51	361.59	929726.8	0.1137	1.34
357	0.5	47	1.5	53	362.76	929726.8	0.1137	1.49
358	-0.5	45	0.5	57	363.41	929726.8	0.1137	1.00

359	-1.5	40	-0.5	56	364.04	929726.8	0.1137	1.07
360	0.5	49	1.5	51	638.49	885606.8	0.0311	0.46
361	-0.5	49	0.5	54	639.37	885606.8	0.0311	1.54
362	-1.5	44	-0.5	54	640.21	885606.8	0.0311	0.54
363	1.5	44	2.5	45	641.29	885606.8	0.0311	1.95
364	0.5	48	1.5	52	642.17	885606.8	0.0311	2.85
365	-0.5	48	0.5	55	643.06	885606.8	0.0311	4.04

[a] Note that $M_F = M_J + M_I\,(^1\mathrm{H}) + M_I\,(^{14}\mathrm{N})$.

[b] The rotational quantum numbers used to determine the eigenstates for odd N were (1, 5, 0, 6) for (N_{min}, N_{max}, J_{min}, J_{max}).

[c] The rotational quantum numbers used to determine the eigenstates for even N were (0, 6, 1, 7) for (N_{min}, N_{max}, J_{min}, J_{max}).

Line	ODD		EVEN		B (mT)	ν_{Laser} (MHz)	Weight	O – C (MHz)
	M_F[a]	Eigenstate[b]	M_F[a]	Eigenstate[c]				
1	1.5	28	1.5	50	440.41	2714714.7	0.0356	2.32
2	0.5	27	0.5	53	442.10	2714714.7	0.0356	1.87
3	-0.5	28	-0.5	53	443.82	2714714.7	0.0356	2.59
4	2.5	29	2.5	44	444.51	2714714.7	0.0356	2.87
5	1.5	29	1.5	49	446.20	2714714.7	0.0356	2.38
6	0.5	28	0.5	52	447.94	2714714.7	0.0355	2.58
7	-0.5	26	-0.5	49	674.71	2714714.7	0.0388	-0.05
8	-1.5	27	-1.5	46	675.44	2714714.7	0.0387	-0.35
9	-2.5	26	-2.5	40	676.10	2714714.7	0.0387	1.79
10	0.5	26	0.5	49	677.43	2714714.7	0.0387	1.15
11	-0.5	27	-0.5	48	678.14	2714714.7	0.0387	2.38
12	-1.5	28	-1.5	45	678.88	2714714.7	0.0355	1.66
13	-1.5	22	-1.5	40	843.50	2714714.7	0.0342	0.03
14	-2.5	20	-2.5	37	843.95	2714714.7	0.0342	0.75
15	-3.5	18	-3.5	33	844.40	2714714.7	0.0343	1.20
16	-0.5	24	-0.5	42	846.03	2714714.7	0.0342	-1.34
17	-1.5	23	-1.5	41	846.46	2714714.7	0.0343	-0.32
18	-2.5	21	-2.5	38	846.91	2714714.7	0.0343	0.29
19	3.5	19	3.5	34	1080.49	2714714.7	0.0505	1.37
20	2.5	22	2.5	39	1084.51	2714714.7	0.0508	0.80
21	3.5	20	3.5	35	1091.39	2714714.7	0.0510	2.13
22	2.5	23	2.5	40	1095.45	2714714.7	0.0513	2.56
23	-1.5	25	-2.5	44	299.71	2714714.7	0.0149	1.33
24	-2.5	24	-3.5	36	301.22	2714714.7	0.0149	1.73
25	-3.5	21	-4.5	27	302.75	2714714.7	0.0149	2.26
26	-0.5	25	-1.5	50	303.49	2714714.7	0.0149	1.32
27	-1.5	26	-2.5	43	304.99	2714714.7	0.0149	2.17
28	-2.5	25	-3.5	35	306.55	2714714.7	0.0149	1.47
29	0.5	29	1.5	50	481.39	2714714.7	0.0604	-2.69
30	-0.5	29	0.5	53	482.97	2714714.7	0.0603	-3.11
31	-1.5	29	-0.5	53	484.64	2714714.7	0.0602	-3.28
32	1.5	30	2.5	44	485.34	2714714.7	0.0603	-3.04
33	0.5	30	1.5	49	486.89	2714714.7	0.0602	-2.86
34	-0.5	30	0.5	52	488.56	2714714.7	0.0602	-3.08
35	-0.5	26	0.5	51	603.20	2714714.7	0.0679	0.81
36	-1.5	27	-0.5	51	604.10	2714714.7	0.0677	1.44
37	-2.5	26	-1.5	47	605.05	2714714.7	0.0677	1.80
38	0.5	26	1.5	48	606.26	2714714.7	0.0677	1.18
39	-0.5	27	0.5	50	607.21	2714714.7	0.0676	1.37
40	-1.5	28	-0.5	50	608.13	2714714.7	0.0676	1.75
41	-1.5	22	-1.5	49	503.06	2742946.0	0.0174	0.26
42	-2.5	20	-2.5	42	503.99	2742946.0	0.0174	-1.41
43	-3.5	18	-3.5	34	504.88	2742946.0	0.0174	-2.55

44	-0.5	24	-0.5	52	506.07	2742946.0	0.0174	-1.66
45	-1.5	23	-1.5	48	506.96	2742946.0	0.0173	-1.79
46	-2.5	21	-2.5	41	507.82	2742946.0	0.0174	-1.96
47	-2.5	22	-2.5	44	559.16	2742946.0	0.0322	-3.07
48	-3.5	19	-3.5	36	560.61	2742946.0	0.0322	-2.43
49	-4.5	15	-4.5	27	562.11	2742946.0	0.0322	-2.78
50	-1.5	24	-1.5	50	562.86	2742946.0	0.0322	-2.05
51	-2.5	23	-2.5	43	564.36	2742946.0	0.0322	-2.47
52	-3.5	20	-3.5	35	565.83	2742946.0	0.0322	-2.28
53	-1.5	22	-2.5	44	416.96	2742946.0	0.0159	0.66
54	-2.5	20	-3.5	36	418.01	2742946.0	0.0159	0.71
55	-3.5	18	-4.5	27	419.06	2742946.0	0.0159	1.47
56	-0.5	24	-1.5	50	420.18	2742946.0	0.0159	0.22
57	-1.5	23	-2.5	43	421.22	2742946.0	0.0159	0.66
58	-2.5	21	-3.5	35	422.32	2742946.0	0.0159	-0.55
59	-0.5	22	-1.5	49	446.81	2742946.0	0.0154	-0.41
60	-1.5	20	-2.5	42	447.54	2742946.0	0.0154	-0.84
61	-2.5	19	-3.5	34	448.27	2742946.0	0.0154	-1.11
62	0.5	24	-0.5	52	449.59	2742946.0	0.0154	-1.06
63	-0.5	23	-1.5	48	450.29	2742946.0	0.0154	-0.19
64	-1.5	21	-2.5	41	451.02	2742946.0	0.0154	-0.62
65	0.5	22	-0.5	49	492.52	2742946.0	0.0059	0.40
66	-0.5	20	-1.5	46	492.84	2742946.0	0.0059	0.84
67	-1.5	19	-2.5	40	493.13	2742946.0	0.0059	2.86
68	1.5	23	0.5	49	494.82	2742946.0	0.0059	-0.31
69	0.5	23	-0.5	48	495.16	2742946.0	0.0059	-0.10
70	-0.5	21	-1.5	45	495.45	2742946.0	0.0059	1.34
71	-2.5	22	-1.5	49	734.62	2742946.0	0.0344	-0.52
72	-3.5	19	-2.5	42	735.80	2742946.0	0.0344	-0.79
73	-4.5	15	-3.5	34	736.89	2742946.0	0.0344	-0.30
74	-1.5	24	-0.5	52	737.88	2742946.0	0.0344	0.39
75	-2.5	23	-1.5	48	739.12	2742946.0	0.0344	-0.75
76	-3.5	20	-2.5	41	740.25	2742946.0	0.0344	-1.61
77	-1.5	22	-0.5	49	590.98	2742946.0	0.0173	3.24
78	-2.5	20	-1.5	46	591.61	2742946.0	0.0173	2.55
79	-3.5	18	-2.5	40	592.17	2742946.0	0.0173	3.22
80	-0.5	24	0.5	49	593.61	2742946.0	0.0173	2.75
81	-1.5	23	-0.5	48	594.22	2742946.0	0.0173	3.46
82	-2.5	21	-1.5	45	594.78	2742946.0	0.0173	3.42
83	2.5	34	1.5	45	53.84	1799139.3	0.0829	0.14
84	1.5	39	0.5	44	54.71	1799139.3	0.0826	-0.50
85	0.5	42	-0.5	43	55.61	1799139.3	0.0825	0.82
86	3.5	27	2.5	43	56.40	1799139.3	0.0834	-0.07
87	2.5	35	1.5	46	57.32	1799139.3	0.0831	0.30
88	1.5	40	0.5	45	58.19	1799139.3	0.0830	1.07

89	1.5	41	0.5	46	73.27	1799139.3	0.1293	0.29
90	0.5	43	-0.5	44	74.21	1799139.3	0.1293	0.04
91	-0.5	42	-1.5	42	75.19	1799139.3	0.1291	0.82
92	2.5	36	1.5	47	76.05	1799139.3	0.1298	0.24
93	1.5	42	0.5	47	77.04	1799139.3	0.1297	0.72
94	0.5	44	-0.5	45	77.97	1799139.3	0.1296	0.80
95	-1.5	43	-0.5	49	102.34	1799139.3	0.0275	-0.37
96	-2.5	36	-1.5	48	103.74	1799139.3	0.0276	0.07
97	-3.5	27	-2.5	44	105.24	1799139.3	0.0276	-1.96
98	-0.5	47	0.5	49	105.98	1799139.3	0.0276	-2.02
99	-1.5	42	-0.5	50	107.36	1799139.3	0.0276	-0.77
100	-2.5	35	-1.5	49	108.84	1799139.3	0.0276	-1.99
101	0.5	45	-0.5	47	114.32	1799139.3	0.1084	0.86
102	-0.5	43	-1.5	44	115.45	1799139.3	0.1084	0.88
103	-1.5	39	-2.5	39	116.68	1799139.3	0.1085	1.58
104	1.5	43	0.5	48	117.40	1799139.3	0.1085	0.34
105	0.5	46	-0.5	46	118.58	1799139.3	0.1089	0.79
106	-0.5	44	-1.5	43	119.76	1799139.3	0.1087	1.05
107	0.5	45	-0.5	46	285.20	1799139.3	0.0690	-0.77
108	-0.5	43	-1.5	43	286.86	1799139.3	0.0689	-0.90
109	-1.5	39	-2.5	39	288.47	1799139.3	0.0689	-1.20
110	1.5	43	0.5	48	288.95	1799139.3	0.0689	-0.19
111	0.5	46	-0.5	47	290.64	1799139.3	0.0689	-0.87
112	-0.5	44	-1.5	44	292.17	1799139.3	0.0695	-0.15
113	2.5	34	1.5	45	78.30	1798647.0	0.0802	-1.70
114	1.5	39	0.5	44	79.16	1798647.0	0.0799	-1.93
115	0.5	42	-0.5	43	79.99	1798647.0	0.0799	-1.33
116	3.5	27	2.5	43	80.97	1798647.0	0.0802	-1.38
117	2.5	35	1.5	46	81.83	1798647.0	0.0801	-1.59
118	1.5	40	0.5	45	82.66	1798647.0	0.0801	-0.96
119	-1.5	43	-0.5	49	89.89	1798647.0	0.0170	1.12
120	-2.5	36	-1.5	48	91.28	1798647.0	0.0170	1.68
121	-3.5	27	-2.5	44	92.75	1798647.0	0.0170	0.64
122	-0.5	47	0.5	49	93.48	1798647.0	0.0171	0.73
123	-1.5	42	-0.5	50	94.93	1798647.0	0.0170	-1.08
124	-2.5	35	-1.5	49	96.30	1798647.0	0.0171	1.87
125	1.5	41	0.5	46	107.05	1798647.0	0.1282	-0.96
126	0.5	43	-0.5	44	108.03	1798647.0	0.1282	-0.42
127	-0.5	42	-1.5	42	108.94	1798647.0	0.1280	-0.31
128	2.5	36	1.5	47	109.90	1798647.0	0.1284	-0.94
129	1.5	42	0.5	47	110.89	1798647.0	0.1283	-0.24
130	0.5	44	-0.5	45	111.83	1798647.0	0.1280	0.32
131	0.5	39	-0.5	58	1166.31	973224.3	0.0061	-2.10
132	-0.5	38	-1.5	53	1167.01	973224.3	0.0061	-2.34
133	-1.5	36	-2.5	45	1167.70	973224.3	0.0061	-0.94

134	1.5	38	0.5	58	1168.99	973224.3	0.0061	3.00
135	0.5	40	-0.5	57	1169.88	973224.3	0.0061	-5.06
136	-0.5	39	-1.5	52	1170.57	973224.3	0.0061	-5.63
137	0.5	39	-0.5	58	1583.36	995077.8	0.0057	-0.71
138	-0.5	38	-1.5	53	1584.09	995077.8	0.0057	-1.74
139	-1.5	36	-2.5	45	1584.82	995077.8	0.0057	1.19
140	1.5	38	0.5	58	1586.17	995077.8	0.0057	1.48
141	0.5	40	-0.5	57	1586.83	995077.8	0.0057	8.98
142	-0.5	39	-1.5	52	1587.56	995077.8	0.0057	7.11
143	0.5	49	1.5	51	1591.59	802492.8	0.0066	-2.20
144	-0.5	49	0.5	54	1592.45	802492.8	0.0065	-2.02
145	-1.5	44	-0.5	54	1593.38	802492.8	0.0066	-0.19
146	1.5	44	2.5	45	1594.57	802492.8	0.0065	-2.72
147	0.5	48	1.5	52	1595.48	802492.8	0.0066	-1.21
148	-0.5	48	0.5	55	1596.35	802492.8	0.0066	-1.21
149	0.5	45	1.5	51	366.47	885606.8	0.0285	-0.04
150	-0.5	43	0.5	54	366.99	885606.8	0.0285	0.49
151	-1.5	39	-0.5	54	367.46	885606.8	0.0285	0.33
152	1.5	43	2.5	45	368.95	885606.8	0.0285	0.51
153	0.5	46	1.5	52	369.52	885606.8	0.0285	2.83
154	-0.5	44	0.5	55	369.99	885606.8	0.0285	2.56
155	1.5	41	1.5	51	625.58	885606.8	0.0649	-0.32
156	0.5	43	0.5	54	625.85	885606.8	0.0649	-0.85
157	-0.5	42	-0.5	54	626.21	885606.8	0.0649	0.10
158	2.5	36	2.5	45	627.86	885606.8	0.0649	0.45
159	1.5	42	1.5	52	628.13	885606.8	0.0649	-0.28
160	0.5	44	0.5	55	628.46	885606.8	0.0650	0.21
161	-0.5	40	-0.5	58	1710.62	960791.1	0.0000	-5.55
162	-1.5	37	-1.5	53	1711.53	960791.1	0.0000	-5.41
163	-2.5	33	-2.5	45	1712.39	960791.1	0.0234	1.38
164	0.5	42	0.5	58	1713.61	960791.1	0.0234	1.10
165	-0.5	41	-0.5	57	1714.55	960791.1	0.0000	6.48
166	-1.5	38	-1.5	52	1715.41	960791.1	0.0000	7.25
167	0.5	39	-0.5	58	921.04	960791.1	0.0068	2.10
168	-0.5	38	-1.5	53	921.74	960791.1	0.0068	1.31
169	-1.5	36	-2.5	45	922.45	960791.1	0.0068	0.26
170	1.5	38	0.5	58	923.84	960791.1	0.0068	-0.51
171	0.5	40	-0.5	57	924.62	960791.1	0.0068	-4.21
172	-0.5	39	-1.5	52	925.20	960791.1	0.0068	0.12
173	-0.5	46	0.5	56	624.60	885606.8	0.0651	0.57
174	-1.5	41	-0.5	55	625.13	885606.8	0.0650	1.11
175	-2.5	34	-1.5	51	625.51	885606.8	0.0649	-1.02
176	0.5	47	1.5	53	627.07	885606.8	0.0650	0.12
177	-0.5	45	0.5	57	627.62	885606.8	0.0649	0.61
178	-1.5	40	-0.5	56	628.10	885606.8	0.0648	1.19

179	0.5	39	-0.5	58	227.30	929726.8	0.1138	-1.20
180	-0.5	38	-1.5	53	227.93	929726.8	0.1138	-0.53
181	-1.5	36	-2.5	45	228.58	929726.8	0.1138	-1.43
182	1.5	38	0.5	58	229.99	929726.8	0.1138	-1.97
183	0.5	40	-0.5	57	230.64	929726.8	0.1138	-2.01
184	-0.5	39	-1.5	52	231.25	929726.8	0.1138	-1.51
185	-0.5	37	-1.5	51	431.77	929726.8	0.0664	-0.96
186	0.5	37	-0.5	55	432.30	929726.8	0.0664	-0.88
187	1.5	37	0.5	57	433.42	929726.8	0.0664	0.50
188	2.5	33	1.5	53	434.07	929726.8	0.0664	-0.82
189	-0.5	40	-0.5	58	429.60	929726.8	0.0667	1.85
190	-1.5	37	-1.5	53	431.14	929726.8	0.0667	0.85
191	-2.5	33	-2.5	45	432.64	929726.8	0.0667	1.07
192	0.5	41	0.5	58	433.40	929726.8	0.0667	1.33
193	-0.5	41	-0.5	57	434.86	929726.8	0.0667	2.42
194	-1.5	38	-1.5	52	436.36	929726.8	0.0667	2.05
195	1.5	36	1.5	50	642.19	1745439.5	0.0220	3.11
196	0.5	37	0.5	53	642.65	1745439.5	0.0220	1.88
197	-0.5	37	-0.5	53	643.23	1745439.5	0.0220	1.71
198	2.5	33	2.5	44	644.74	1745439.5	0.0220	2.00
199	1.5	37	1.5	49	645.25	1745439.5	0.0221	0.93
200	0.5	38	0.5	52	645.83	1745439.5	0.0221	2.92
201	0.5	39	0.5	51	896.52	1745439.5	0.0139	2.84
202	-0.5	38	-0.5	51	897.12	1745439.5	0.0139	3.14
203	-1.5	36	-1.5	47	897.68	1745439.5	0.0139	1.39
204	1.5	38	1.5	48	899.15	1745439.5	0.0139	2.09
205	0.5	40	0.5	50	899.73	1745439.5	0.0139	-0.26
206	-0.5	39	-0.5	50	900.31	1745439.5	0.0139	0.62
207	0.5	39	0.5	47	1553.63	1745439.5	0.0210	1.23
208	-0.5	38	-0.5	46	1554.41	1745439.5	0.0210	0.91
209	-1.5	36	-1.5	44	1555.12	1745439.5	0.0210	0.44
210	1.5	38	1.5	47	1556.45	1745439.5	0.0210	0.79
211	0.5	40	0.5	48	1557.27	1745439.5	0.0210	1.03
212	-0.5	39	-0.5	47	1557.95	1745439.5	0.0210	0.27
213	1.5	41	1.5	50	1728.86	1745439.5	0.0171	1.80
214	0.5	43	0.5	53	1730.27	1745439.5	0.0171	2.25
215	-0.5	42	-0.5	53	1731.69	1745439.5	0.0171	2.32
216	2.5	36	2.5	44	1732.52	1745439.5	0.0171	1.67
217	1.5	42	1.5	49	1733.91	1745439.5	0.0171	1.39
218	0.5	44	0.5	52	1735.35	1745439.5	0.0171	2.21
219	-0.5	40	-0.5	49	1790.01	1745439.5	0.0000	26.20
220	-1.5	37	-1.5	46	1790.51	1745439.5	0.0000	26.60
221	-2.5	33	-2.5	40	1790.97	1745439.5	0.0014	2.52
222	0.5	42	0.5	49	1792.52	1745439.5	0.0014	3.30
223	-0.5	41	-0.5	48	1793.05	1745439.5	0.0000	-20.30

224	-1.5	38	-1.5	45	1793.48	1745439.5	0.0000	-21.20
225	0.5	39	-0.5	44	1719.79	1745439.5	0.0145	-0.42
226	-0.5	38	-1.5	42	1720.30	1745439.5	0.0145	-0.94
227	-1.5	36	-2.5	39	1720.81	1745439.5	0.0145	-0.35
228	1.5	38	0.5	46	1722.28	1745439.5	0.0145	-1.16
229	0.5	40	-0.5	45	1722.83	1745439.5	0.0145	-1.01
230	-0.5	39	-1.5	43	1723.31	1745439.5	0.0145	-0.82
231	0.5	39	-0.5	49	921.96	1745439.5	0.0071	-5.24
232	-0.5	38	-1.5	46	922.53	1745439.5	0.0071	-2.94
233	-1.5	36	-2.5	40	923.01	1745439.5	0.0071	-5.98
234	1.5	38	0.5	49	924.50	1745439.5	0.0071	-6.27
235	0.5	40	-0.5	48	925.07	1745439.5	0.0071	-7.08
236	-0.5	39	-1.5	45	925.53	1745439.5	0.0071	-8.01
237	0.5	39	1.5	50	757.40	1745439.5	0.0232	-3.21
238	-0.5	38	0.5	53	758.53	1745439.5	0.0232	-2.80
239	-1.5	36	-0.5	53	759.61	1745439.5	0.0232	-4.91
240	1.5	38	2.5	44	760.72	1745439.5	0.0232	-2.61
241	0.5	40	1.5	49	761.85	1745439.5	0.0232	-2.30
242	-0.5	39	0.5	52	762.95	1745439.5	0.0232	-3.38
243	-1.5	43	-0.5	40	342.21	1838839.3	0.0302	-0.55
244	-2.5	36	-1.5	38	343.17	1838839.3	0.0301	-0.07
245	-3.5	27	-2.5	36	344.15	1838839.3	0.0301	0.31
246	-0.5	47	0.5	42	345.28	1838839.3	0.0301	0.81
247	-1.5	42	-0.5	41	346.24	1838839.3	0.0301	1.30
248	-2.5	35	-1.5	39	347.24	1838839.3	0.0300	0.89
249	-0.5	46	0.5	40	400.80	1838839.3	0.0316	0.49
250	-1.5	41	-0.5	38	401.35	1838839.3	0.0316	-1.46
251	-2.5	34	-1.5	37	401.84	1838839.3	0.0316	-1.40
252	0.5	47	1.5	41	403.33	1838839.3	0.0316	-1.42
253	-0.5	45	0.5	41	403.83	1838839.3	0.0316	-1.37
254	-1.5	40	-0.5	39	404.32	1838839.3	0.0315	-1.54
255	0.5	45	-0.5	40	748.85	1838839.3	0.0563	1.65
256	-0.5	43	-1.5	38	749.43	1838839.3	0.0563	0.93
257	-1.5	39	-2.5	36	749.88	1838839.3	0.0563	1.25
258	1.5	43	0.5	42	751.36	1838839.3	0.0563	1.28
259	0.5	46	-0.5	41	751.98	1838839.3	0.0564	-0.76
260	-0.5	44	-1.5	39	752.41	1838839.3	0.0564	0.34
261	-0.5	46	-1.5	40	778.42	1838839.3	0.0818	-1.56
262	-1.5	41	-2.5	37	779.30	1838839.3	0.0816	-0.68
263	-2.5	34	-3.5	33	780.16	1838839.3	0.0815	-0.29
264	0.5	47	-0.5	42	781.40	1838839.3	0.0816	-0.71
265	-0.5	45	-1.5	41	782.31	1838839.3	0.0815	0.94
266	-1.5	40	-2.5	38	783.10	1838839.3	0.0813	1.34
267	0.5	49	-0.5	44	972.11	1838839.3	0.0847	-1.19
268	-0.5	49	-1.5	42	973.90	1838839.3	0.0846	-1.30

269	-1.5	44	-2.5	39	975.68	1838839.3	0.0845	-0.10
270	1.5	44	0.5	46	976.28	1838839.3	0.0846	-1.05
271	0.5	48	-0.5	45	978.02	1838839.3	0.0845	-0.05
272	-0.5	48	-1.5	43	979.83	1838839.3	0.0844	0.36
273	-0.5	40	-0.5	40	1585.36	1838839.3	0.0120	-1.54
274	-1.5	37	-1.5	38	1585.83	1838839.3	0.0120	2.36
275	-2.5	33	-2.5	36	1586.51	1838839.3	0.0120	0.04
276	0.5	42	0.5	42	1587.98	1838839.3	0.0120	-1.09
277	-0.5	41	-0.5	41	1588.56	1838839.3	0.0120	-0.23
278	-1.5	38	-1.5	39	1589.17	1838839.3	0.0120	-0.59
279	0.5	49	0.5	47	1147.88	1838839.3	0.0229	1.07
280	-0.5	49	-0.5	46	1149.21	1838839.3	0.0334	-0.33
281	-1.5	44	-1.5	44	1150.52	1838839.3	0.0334	0.47
282	1.5	44	1.5	47	1151.52	1838839.3	0.0334	-0.79
283	0.5	48	0.5	48	1152.79	1838839.3	0.0334	-1.01
284	-0.5	48	-0.5	47	1154.12	1838839.3	0.0334	-0.65
285	-1.5	43	-1.5	40	491.80	1838839.3	0.0644	-0.28
286	-2.5	36	-2.5	37	493.28	1838839.3	0.0644	0.03
287	-3.5	27	-3.5	33	494.76	1838839.3	0.0644	0.64
288	-0.5	47	-0.5	42	495.60	1838839.3	0.0644	-1.06
289	-1.5	42	-1.5	41	497.00	1838839.3	0.0643	1.36
290	-2.5	35	-2.5	38	498.58	1838839.3	0.0643	-0.66
291	-0.5	46	-0.5	40	469.34	1838839.3	0.0355	2.35
292	-1.5	41	-1.5	38	470.05	1838839.3	0.0354	3.12
293	-2.5	34	-2.5	36	470.79	1838839.3	0.0354	1.53
294	0.5	47	0.5	42	472.08	1838839.3	0.0354	2.98
295	-0.5	45	-0.5	41	472.89	1838839.3	0.0354	0.55
296	-1.5	40	-1.5	39	473.58	1838839.3	0.0355	0.41
297	0.5	49	0.5	40	624.92	1868475.5	0.0282	-0.60
298	-0.5	49	-0.5	38	625.64	1868475.5	0.0281	-1.28
299	-1.5	44	-1.5	37	626.35	1868475.5	0.0282	-0.49
300	1.5	44	1.5	41	627.69	1868475.5	0.0281	-0.04
301	0.5	48	0.5	41	628.37	1868475.5	0.0282	0.86
302	-0.5	48	-0.5	39	629.12	1868475.5	0.0281	0.04
303	-0.5	46	-0.5	40	1160.28	1868475.5	0.0066	-4.35
304	-1.5	41	-1.5	38	1160.91	1868475.5	0.0066	-5.56
305	-2.5	34	-2.5	36	1161.48	1868475.5	0.0222	-0.51
306	0.5	47	0.5	42	1162.94	1868475.5	0.0222	-1.55
307	-0.5	45	-0.5	41	1163.53	1868475.5	0.0066	4.78
308	-1.5	40	-1.5	39	1164.16	1868475.5	0.0066	1.60
309	-1.5	43	-1.5	40	1657.77	1868475.5	0.0218	0.84
310	-2.5	36	-2.5	37	1658.93	1868475.5	0.0218	1.69
311	-3.5	27	-3.5	33	1660.17	1868475.5	0.0218	1.59
312	-0.5	47	-0.5	42	1661.11	1868475.5	0.0218	3.20
313	-1.5	42	-1.5	41	1662.30	1868475.5	0.0218	4.70

314	-2.5	35	-2.5	38	1663.51	1868475.5	0.0218	3.91
315	-0.5	46	0.5	39	1067.53	1868475.5	0.0066	-4.31
316	-1.5	41	-0.5	38	1067.91	1868475.5	0.0066	-5.74
317	-2.5	34	-1.5	37	1068.24	1868475.5	0.0066	-0.68
318	0.5	47	1.5	39	1069.85	1868475.5	0.0066	-0.56
319	-0.5	45	0.5	40	1070.23	1868475.5	0.0066	2.70
320	-1.5	40	-0.5	39	1070.54	1868475.5	0.0066	4.25
321	0.5	49	-0.5	40	730.12	1868475.5	0.0284	3.07
322	-0.5	49	-1.5	38	731.23	1868475.5	0.0284	1.36
323	-1.5	44	-2.5	36	732.26	1868475.5	0.0284	1.89
324	1.5	44	0.5	42	733.39	1868475.5	0.0284	1.14
325	0.5	48	-0.5	41	734.47	1868475.5	0.0284	0.48
326	-0.5	48	-1.5	39	735.56	1868475.5	0.0284	-1.04
327	-1.5	22	-1.5	49	796.76	2754995.7	0.0193	0.60
328	-2.5	20	-2.5	42	797.60	2754995.7	0.0193	0.12
329	-3.5	18	-3.5	34	798.42	2754995.7	0.0193	-0.46
330	-0.5	24	-0.5	52	799.66	2754995.7	0.0193	0.71
331	-1.5	23	-1.5	48	800.50	2754995.7	0.0193	0.67
332	-2.5	21	-2.5	41	801.29	2754995.7	0.0193	0.96
333	-2.5	22	-2.5	44	1032.65	2754995.7	0.0184	2.78
334	-3.5	19	-3.5	36	1034.00	2754995.7	0.0184	3.16
335	-4.5	15	-4.5	27	1035.37	2754995.7	0.0184	3.30
336	-1.5	24	-1.5	50	1036.27	2754995.7	0.0184	2.47
337	-2.5	23	-2.5	43	1037.64	2754995.7	0.0184	2.64
338	-3.5	20	-3.5	35	1039.06	2754995.7	0.0184	1.15
339	-1.5	22	-2.5	44	699.29	2754995.7	0.0020	-2.91
340	-2.5	20	-3.5	36	700.25	2754995.7	0.0020	-1.03
341	-3.5	18	-4.5	27	701.32	2754995.7	0.0020	-3.81
342	-0.5	24	-1.5	50	702.46	2754995.7	0.0020	-4.15
343	-1.5	23	-2.5	43	703.46	2754995.7	0.0020	-4.02
344	-2.5	21	-3.5	35	704.46	2754995.7	0.0020	-3.68
345	-0.5	22	-1.5	49	726.16	2754995.7	0.0183	-1.72
346	-1.5	20	-2.5	42	726.81	2754995.7	0.0183	-1.67
347	-2.5	19	-3.5	34	727.47	2754995.7	0.0183	-1.76
348	0.5	24	-0.5	52	728.83	2754995.7	0.0183	-0.65
349	-0.5	23	-1.5	48	729.51	2754995.7	0.0183	-1.47
350	-1.5	21	-2.5	41	730.17	2754995.7	0.0183	-2.10
351	0.5	21	-0.5	49	773.58	2754995.7	0.0021	-5.33
352	-0.5	20	-1.5	46	773.86	2754995.7	0.0021	-4.43
353	-1.5	19	-2.5	40	774.14	2754995.7	0.0021	-1.62
354	1.5	21	0.5	49	775.85	2754995.7	0.0021	-4.67
355	0.5	22	-0.5	48	776.16	2754995.7	0.0021	-3.02
356	-0.5	21	-1.5	45	776.46	2754995.7	0.0021	-3.22
357	-0.5	22	0.5	51	780.00	2754995.7	0.0075	-2.73
358	-1.5	20	-0.5	51	780.50	2754995.7	0.0075	-3.37

359	-2.5	19	-1.5	47	780.94	2754995.7	0.0075	-0.57
360	0.5	24	1.5	48	782.49	2754995.7	0.0075	-1.56
361	-0.5	23	0.5	50	782.98	2754995.7	0.0075	-0.45
362	-1.5	21	-0.5	50	783.47	2754995.7	0.0075	-1.15
363	-1.5	22	-0.5	49	883.32	2754995.7	0.0194	-5.19
364	-2.5	20	-1.5	46	883.94	2754995.7	0.0194	-5.93
365	-3.5	18	-2.5	40	884.46	2754995.7	0.0196	-1.73
366	-0.5	24	0.5	49	885.91	2754995.7	0.0195	-2.21
367	-1.5	23	-0.5	48	886.53	2754995.7	0.0196	-0.34
368	-2.5	21	-1.5	45	887.17	2754995.7	0.0194	-4.07

[a] Note that $M_F = M_J + M_I\,(^1\mathrm{H}) + M_I\,(^{14}\mathrm{N})$.

[b] The rotational quantum numbers used to determine the eigenstates for odd N were (1, 5, 0, 6) for (N_{min}, N_{max}, J_{min}, J_{max}).

[c] The rotational quantum numbers used to determine the eigenstates for even N were (0, 6, 1, 7) for (N_{min}, N_{max}, J_{min}, J_{max}).